

Acid sphingomyelinase regulates glucose and lipid metabolism in hepatocytes through AKT activation and AMP-activated protein kinase suppression

Yosuke Osawa,^{*,†,1} Ekihiro Seki,[§] Yuzo Kodama,[§] Atsushi Suetsugu,[†] Kouichi Miura,[§] Masayuki Adachi,[§] Hiroyasu Ito,^{*} Yoshimune Shiratori,[†] Yoshiko Banno,[‡] Jerrold M. Olefsky,[§] Masahito Nagaki,[†] Hisataka Moriwaki,[†] David A. Brenner,[§] and Mitsuru Seishima^{*}

^{*}Department of Informative Clinical Medicine, [†]Department of Gastroenterology, and [‡]Department of Cell Signaling, Gifu University Graduate School of Medicine, Gifu, Japan; and [§]Department of Medicine, University of California–San Diego School of Medicine, La Jolla, California USA

ABSTRACT Acid sphingomyelinase (ASM) regulates the homeostasis of sphingolipids, including ceramides and sphingosine-1-phosphate (SIP). Because sphingolipids regulate AKT activation, we investigated the role of ASM in hepatic glucose and lipid metabolism. Initially, we overexpressed ASM in the livers of wild-type and diabetic *db/db* mice by adenovirus vector (Ad5ASM). In these mice, glucose tolerance was improved, and glycogen and lipid accumulation in the liver were increased. Using primary cultured hepatocytes, we confirmed that ASM increased glucose uptake, glycogen deposition, and lipid accumulation through activation of AKT and glycogen synthase kinase-3 β . In addition, ASM induced up-regulation of glucose transporter 2 accompanied by suppression of AMP-activated protein kinase (AMPK) phosphorylation. Loss of sphingosine kinase-1 (SphK1) diminished ASM-mediated AKT phosphorylation, but exogenous SIP induced AKT activation in hepatocytes. In contrast, SphK1 deficiency did not affect AMPK activation. These results suggest that the SphK/SIP pathway is required for ASM-mediated AKT activation but not for AMPK inactivation. Finally, we found that treatment with high-dose glucose increased glycogen deposition and lipid accumulation in wild-type hepatocytes but not in ASM^{-/-} cells. This result is consistent with glucose intolerance in ASM^{-/-} mice. In conclusion, ASM modulates AKT activation and AMPK inactivation, thus regulating glucose and lipid metabolism in the liver.—Osawa, Y., Seki, E., Kodama, Y., Suetsugu, A., Miura, K., Adachi, M., Ito, H., Shiratori, Y., Banno, Y., Olefsky, J. M., Nagaki, M., Moriwaki, H., Brenner, D. A., Seishima, M. Acid sphingomyelinase regulates glucose and lipid metabolism in hepatocytes through AKT activation and AMP-activated protein kinase suppression. *FASEB J.* 25, 1133–1144 (2011). www.fasebj.org

Key Words: sphingosine-1-phosphate • glucose intolerance • glucose transporter 2 • glycogen synthase kinase-3 β

THE LIVER IS A KEY ORGAN for glucose and lipid metabolism. During feeding, hepatocytes increase glucose uptake in response to elevated glucose levels in the

portal vein and increase glycogen and triacylglyceride synthesis. AKT is a key molecule for insulin signaling and glucose metabolism. On AKT activation, glucose influx is stimulated by activation of glycogen synthesis through glycogen synthase kinase (GSK)-3 β . The facilitative glucose transporter (GLUT) 2 is predominantly expressed in the liver (1). Hepatic GLUT2 is located at the plasma membrane even in the absence of insulin stimulation; glucose uptake by GLUT2 is therefore not directly affected by insulin. Glucose increases GLUT2 mRNA levels in hepatocytes (2), resulting in increased glucose influx. Constitutive activity of AMP-activated protein kinase (AMPK) decreases glycogen synthesis accompanied by down-regulation of GLUT2 expression (3). Therefore, both AKT and AMPK are involved in glucose metabolism.

Acid sphingomyelinase (ASM) deficiency leads to Niemann-Pick disease. ASM has been reported to be involved in various cellular functions (4), including glucose and lipid metabolism. ASM activity is increased in the serum of type 2 diabetic patients (5). Sphingomyelinase induces GLUT4 translocation to the plasma membrane (6, 7) and increases glucose uptake by adipocytes (7, 8). A high-fat, high-cholesterol diet does not induce hepatic triacylglyceride accumulation in ASM-deficient mice (ASM^{-/-}) under an LDL receptor-deficient condition (9). ASM hydrolyzes sphingomyelin to ceramide and phosphorylcholine. Ceramide has been identified as a bioactive mediator in various

¹ Correspondence: Department of Informative Clinical Medicine, Gifu University Graduate School of Medicine, 1-1 Yanagido, Gifu, 501-1194, Japan. E-mail: osawa-gif@umin.ac.jp

This is an Open Access article distributed under the terms of the Creative Commons Attribution Non-Commercial License (<http://creativecommons.org/licenses/by-nc/3.0/us/>) which permits unrestricted non-commercial use, distribution, and reproduction in any medium, provided the original work is properly cited.

doi: 10.1096/fj.10-168351

This article includes supplemental data. Please visit <http://www.fasebj.org> to obtain this information.

cellular functions, including apoptosis and the cell cycle (10, 11). Ceramide accumulation contributes to the development of type 2 diabetes (12). Indeed, inhibition of ceramide synthesis by myriocin, serine palmitoyltransferase inhibitor, or dihydroceramide desaturase improves insulin resistance induced by glucocorticoid or saturated fat (13). Ceramide induces insulin resistance by inactivation of AKT through protein phosphatase-2A and PKC- ζ (14, 15) or by inhibition of AKT translocation to the plasma membrane (16). In addition, ceramide inhibits AMPK activation in hepatoma cells (17).

Not only ceramide but also its metabolite sphingosine-1-phosphate (S1P) is involved in glucose metabolism. Ceramide is hydrolyzed by ceramidase to sphingosine, which is further phosphorylated to S1P by sphingosine kinase (SphK; ref. 18). S1P stimulates AKT activation in human (19) and rodent hepatocytes (20) through the S1P receptor (S1PR). S1P signaling also increases glucose uptake *via* the insulin receptor and production of reactive oxygen species in C2C12 mouse myoblast cells (21). Because sphingolipids are important in glucose and lipid metabolism, we investigated the role of ASM in glucose and lipid metabolism in hepatocytes. In this study, we determined that ASM stimulates glucose uptake, glycogen deposition, and lipid accumulation *via* S1P formation and subsequent AKT activation. As a result, ASM deficiency causes glucose intolerance.

MATERIALS AND METHODS

Animals

The experiments were conducted in accordance with the institutional guidelines of Gifu University and Columbia University. Sprague-Dawley male rats and male wild-type (C57BL/6J), ASM^{-/-}, SphK1-deficient (SphK1^{-/-}; refs. 20, 22), and obese and diabetic *db/db* mice (C57BL/6 background) were used for this study.

Mice

ASM^{-/-} mice (C57BL/6 background) and SphK1^{-/-} mice (C57BL/6 background) (23), which lack the putative lipid kinase catalytic domain, were bred for studies. Obese and diabetic *db/db* mice (C57BL/6 background) were obtained from the Institute for Animal Reproduction (Ibaragi, Japan), and wild-type C57BL/6J mice were from Japan SLC (Shizuoka, Japan). Eight- to 10-wk-old male mice were used for *in vivo* studies.

Intraperitoneal glucose tolerance test (IPGTT)

The 8- to 10-wk-old male mice (wild-type, *db/db*, or ASM^{-/-} mice) were deprived of food for 18 h. D-Glucose (2 mg/g body weight) was injected intraperitoneally, and blood glucose levels were monitored at 0, 30, 60, and 120 min after the injection using G checker (Sanko Junyaku, Tokyo, Japan). Values for area under the blood glucose curve after glucose loading were calculated. Serum insulin content was measured with a mouse insulin ELISA kit (Shibayagi, Gunma, Japan).

Primary hepatocyte cultures

Sprague-Dawley male rats (200–250 g) or mice (4 wk old) were anesthetized with ketamine and xylazine administered by intraperitoneal injection. Hepatocytes were then isolated by a nonrecirculating *in situ* collagenase perfusion of livers cannulating through the portal vein of rats or inferior vena cava of mice. Livers were first perfused *in situ* with 0.5 mM EGTA containing calcium-free salt solution, followed by perfusion with solution containing 0.02% collagenase D (Roche Diagnostics, Indianapolis, IN, USA). The liver was then gently minced on a Petri dish and filtered with polyamide mesh (3-60/42; Sefar America Inc., New York, NY, USA). Hepatocytes were washed 3 times and centrifuged at 50 g for 1 min. Cell viability was consistently >90%, as determined by trypan blue exclusion. Cells were plated on dishes coated with rat collagen type I in Waymouth medium (Invitrogen, Carlsbad, CA, USA) containing 10% fetal bovine serum with antibiotics (plating medium).

Cell treatment

After isolation from rat or mouse livers, hepatocytes were cultured in 10% FBS-containing medium for 4 h. Cells were then washed twice with PBS and changed to serum-free RPMI 1640 (Invitrogen) containing glucose (200 mg/dl) and antibiotics in the presence or absence of recombinant adenoviruses [10 plaque forming units (PFU)/cell]. After a 2-h incubation, the culture medium was changed to serum-free RPMI 1640 containing antibiotics, and the cells were incubated for an additional 16 h. Before stimulation with ASM (1 IU/ml; Sigma-Aldrich, St. Louis, MO, USA), S1P (1 μ M; Sigma-Aldrich), or high-dose glucose (600 mg/dl), the cells were washed twice with PBS. The cells were pretreated with imipramine (50 μ M; Sigma-Aldrich) for 1 h or with pertussis toxin (PTX) (Sigma-Aldrich) for 16 h in some experiments. The hepatocytes were then treated with or without ASM, S1P, or high-dose glucose, and incubated 8 h for glycogen, RNA, and protein extraction or 24 h for Oil Red O staining and triglyceride measurement. The experimental design is shown in Supplemental Fig. S1A.

Recombinant adenoviruses

The adenovirus 5 (Ad5) variants Ad5GFP, Ad5CA-AKT, Ad5DN-AKT, Ad5CA-AMPK, and Ad5DN-AMPK express green fluorescent protein (GFP), constitutively active (CA)-AKT encoding an amino-terminal myristylation signal, dominant-negative (DN)-AKT, *c-myc*-CA-AMPK, and *c-myc*-DN-AMPK, respectively (20, 24). The recombinant replication deficient adenovirus Ad5ASM expressing ASM was constructed by an AdEasy Adenoviral Vector System (Stratagene, La Jolla, CA, USA). In brief, the full length of human ASM DNA was subcloned into pTrack adenoviral vector. The plasmid DNA was prepared by the alkaline lysis method and transfected into BJ5183-AD-1 electroporation-competent cells. The virus was grown in HEK293 cells and purified by banding twice on CsCl gradients, then dialyzed and stored at -20°C . The pTrack plasmid contains a GFP sequence driven under a CMV promoter, and the Ad5ASM expresses both ASM and GFP. Mice were infected with the adenoviruses (5×10^8 PFU/mouse) by intravenous injection. IPGTT was performed on 3 d after the infection. The animals were humanely killed at 3 d for glycogen and protein extraction and at 7 d for Oil Red O staining and triglyceride measurement.

Glucose uptake

Primary cultured hepatocytes were treated with or without ASM for 2 h or infected with Ad5ASM or Ad5GFP, and then

2-deoxy-D-[1-³H]glucose (2 μ Ci/ml; Amersham Biosciences, Piscataway, NJ, USA) was added to the culture medium. After a further 1-h incubation, cells were washed 3 times with ice-cold PBS and lysed in 1% SDS and 200 mM NaOH. The amount of labeled glucose taken up was determined by scintillation counting.

Measurement of glycogen content

After the treatment of hepatocytes for the indicated periods, the dish was placed on ice, washed with ice-cold PBS twice, and then incubated with 30% KOH for 30 min at room temperature. For the measurement of glycogen content in liver tissue, frozen liver tissues were homogenized in 30% KOH. Then, ethanol was added to the lysate, and glycogen was precipitated by centrifugation. The pellet was dissolved with H₂O, and glycogen content was determined by anthrone reagent (2 mg anthrone/ml sulfuric acid). Glucose solution was used as a standard.

Oil Red O staining

For lipid droplet staining, the cells were fixed with 10% formalin and stained with Oil Red O working solution. Hematoxylin was used for counterstaining. For liver tissue, the frozen liver sections were cut at a thickness of 5 μ m on a cryostat and stained with Oil Red O.

Measurement of triglyceride

After the treatment, the primary cultured hepatocytes were washed with PBS and scraped with methanol. For the measurement of triglyceride in liver tissue, frozen liver tissues were homogenized in PBS, and methanol was added to the lysate. The lipids were extracted by the method of Bligh and Dyer (25), and triglyceride content was measured using a triglyceride kit (L-type TG M with lipid calibrator; Wako, Osaka, Japan).

Western blot

For the preparation of total cell proteins, cells or frozen liver tissues were homogenized in radioimmunoprecipitation assay buffer (50 mM Tris-HCl, pH 8.8; 150 mM NaCl; 10 mM EGTA; 1% Triton-X; 0.1% SDS; 1% deoxycholic acid; 0.3 mM PMSF; 1 mM sodium orthovanadate; 10 mM sodium fluoride; 0.1 mM sodium molybdate; and 0.5 mM 4-deoxyypyridoxine). The proteins were separated by SDS-PAGE and were electrophoretically transferred onto nitrocellulose membrane. The membranes were first incubated with the primary antibodies, anti-phosphorylated-AKT (Ser-473; 9271; Cell Signaling Technology, Danvers, MA, USA), AKT (9272; Cell Signaling), phosphorylated-GSK3 β (Ser-9, 9336; Cell Signaling), GSK3 β (610201; BD Biosciences, San Jose, CA, USA), phosphorylated-AMPK α (Thr-172, 2531; Cell Signaling), AMPK α (2603; Cell Signaling), GLUT2 (sc-9116; Santa Cruz Biotechnology, Santa Cruz, CA, USA), ASM (sc-11352; Santa Cruz Biotechnology), and β -actin (Sigma-Aldrich) antibodies. Then, the membrane was incubated with the horseradish peroxidase-coupled secondary antibodies (Santa Cruz Biotechnology). Detection was performed with an ECL system (Amersham Biosciences), and the protein bands were quantified by densitometry using the ImageJ program (U.S. National Institutes of Health; <http://rsb.info.nih.gov/ij/>).

Quantitative real-time RT-PCR

Extracted RNA from the cells was reverse-transcribed, and quantitative real-time PCR with probe-primer sets of GLUT2 and 18S ribosomal RNA (Applied Biosystems, Foster City, CA, USA) was performed using TaqMan analysis (ABI Prism 7000; Applied Biosystems). The changes were normalized based on 18S.

Mass spectrometric analysis of sphingolipids

Electrospray ionization tandem mass spectrometry analysis was performed on a Thermo Finnegan TSQ 7000 triple quadrupole mass spectrometer (Thermo Finnegan, San Jose, CA, USA), operating in multiple reaction monitoring positive ionization mode, as reported previously (26).

SIP formation

Primary rat hepatocytes were incubated with [³H]serine (2 μ Ci/ml)-containing medium for 12 h. Then, the medium was changed to serum-free RPMI 1640 medium containing [³H]serine with subsequent incubation with adenoviruses for an additional 18 h. The cellular lipids were extracted by the method of Bligh and Dyer (25) and separated on TLC plates in the solvent system of 1-butanol/acetic acid/water (60:20:20, v/v). The radiolabeled SIP spot was scraped off from the plates, and the radioactivity was measured in a liquid scintillation counter.

Statistical analysis

The results shown are representative of ≥ 3 independent experiments. Data are expressed as means \pm SD from ≥ 4 independent experiments. Data between groups were analyzed by Student's *t* test. Values of *P* < 0.05 were considered statistically significant.

RESULTS

Exogenous ASM improves glucose metabolism in mice

To explore the role of hepatic ASM on glucose and lipid metabolism, an adenovirus vector expressing human ASM, Ad5ASM, was used in this study. On administration of Ad5ASM into mice, ASM was preferentially expressed in the liver but not in muscle and adipose tissue (Supplemental Fig. S1B, C). As a result, ASM activity in the liver was increased (Supplemental Fig. S1D). Sufficient expression and activity of ASM in Ad5ASM-infected primary cultured hepatocytes were confirmed. This activity efficiently suppressed the level of sphingomyelins in hepatocytes (Supplemental Fig. S1E and Table 1). Initially, we investigated the effect of ASM in a glucose tolerance test and demonstrated that blood glucose levels were decreased in both wild-type (Fig. 1A) and diabetic *db/db* mice (Fig. 1B) in which ASM was overexpressed by Ad5ASM, indicating that ASM improves glucose tolerance. Then, we used primary cultured hepatocytes to investigate the effect of ASM on glucose uptake. Exogenous administration or adenoviral introduction of ASM increased glucose up-

TABLE 1. Changes in the sphingolipid profile in Ad5ASM-infected hepatocytes

Species	Ad5GFP	Ad5ASM
C14-SphM	31.5 ± 0.1	22.2 ± 1.8*
C16-SphM	6626.5 ± 261.3	4376.0 ± 210.8*
C18-SphM	2053.2 ± 65.0	1108.7 ± 53.4*
C18:1-SphM	260.9 ± 5.8	168.7 ± 5.1*
C20-SphM	1062.2 ± 20.0	564.4 ± 84.2*
C20:1-SphM	130.0 ± 2.6	79.3 ± 5.5*
C22-SphM	8397.5 ± 538.7	5223.5 ± 688.8*
C22:1-SphM	1221.8 ± 60.2	696.0 ± 109.1*
C24-SphM	24,630.7 ± 115.6	16,310.1 ± 2479.5*
C24:1-SphM	17,194.4 ± 630.6	10,981.6 ± 1385.0*
C14-Cer	5.8 ± 0.6	7.1 ± 1.5
C16-Cer	181.5 ± 7.5	185.3 ± 4.3
C18-Cer	39.3 ± 5.5	50.4 ± 1.3*
C-18:1-Cer	8.4 ± 0.9	10.1 ± 0.1*
C20-Cer	33.0 ± 5.1	42.8 ± 1.5
C24-Cer	919.8 ± 70.5	1140.7 ± 82.5*
C24:1-Cer	547.0 ± 70.3	598.4 ± 3.8
Sph	140.3 ± 19.0	248.6 ± 14.5*

Primary cultured rat hepatocytes were infected with Ad5GFP or Ad5ASM. Sphingomyelin and the different ceramide species were examined by mass spectrometric analysis. Results are expressed as picomoles lipid per milligram protein; they represent means ± SD from 3 independent experiments. SphM, sphingomyelin; Cer, ceramide; Sph, sphingosine. **P* < 0.05.

take in hepatocytes (Fig. 1C), suggesting that ASM improves glucose tolerance by increased hepatic glucose uptake. Next, we examined the role of ASM in

glycogen synthesis. Exogenous ASM expression increased hepatic glycogen content *in vivo* (Fig. 1D) and *in vitro* (Fig. 1E) using primary cultured hepatocytes. We further examined the role of ASM in lipid metabolism. Exogenous ASM introduction increased hepatic lipid content and serum triglycerides (Fig. 2A, B) *in vivo*. We verified that ASM induces accumulation of lipid droplets and triglyceride in primary cultured hepatocytes (Fig. 2C). These results indicate that ASM contributes not only to glucose uptake but also to the synthesis of glycogen and triglyceride in the liver.

ASM induces AKT activation

AKT is a key molecule in insulin signaling and glucose metabolism. We hypothesized that AKT is involved in ASM-mediated glucose, glycogen, and lipid metabolism. To prove this, we initially investigated whether AKT affects glucose and lipid metabolism in hepatocytes using adenoviral overexpression of DN- or CA-AKT (Ad5DN-AKT and Ad5CA-AKT, respectively). DN-AKT inhibited insulin-induced phosphorylation of AKT, thereby inhibiting glycogen deposition and lipid accumulation by insulin or high-dose glucose in primary cultured hepatocytes (data not shown). In contrast, a constitutively active form of AKT strongly phosphorylated GSK3β (Supplemental Fig. S2A), resulting in increased glycogen deposition and lipid accumulation (Supplemental Fig. S2B and data not shown). AKT is therefore crucial for glucose and lipid

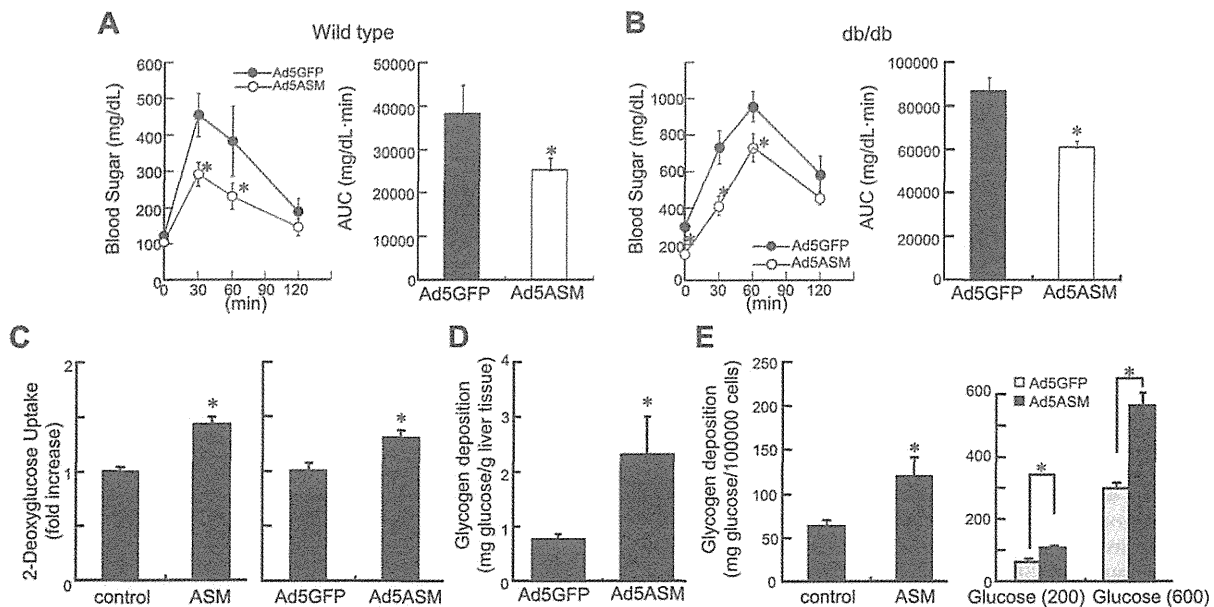


Figure 1. Ad5ASM improves glucose tolerance in mice. *A, B*) Wild-type (*A*) or diabetic *db/db* mice (*B*) were infected with Ad5GFP or Ad5ASM (5×10^6 PFU/mouse), then deprived of food for 18 h, and IPGTT was performed by administering a glucose load of 2 mg/g body weight 3 d after the infection. Values of area under the blood glucose curve were calculated (right panels). *C*) Primary cultured rat hepatocytes were treated with ASM (1 U/ml) for 2 h (left panel) or infected with Ad5GFP or Ad5ASM (10 PFU/cell; right panel), followed by measurement of 2-deoxy-D-[1-³H]glucose uptake after a 1-h incubation period. *D*) Hepatic glycogen content in wild-type mice was determined under food-deprivation conditions at 3 d after the adenoviral infection. *E*) Glycogen content was determined in rat hepatocytes at 8 h after ASM treatment (left panel) or normal (200 mg/dl) and high-dose glucose (600 mg/dl) (right panel) treatment with Ad5GFP or Ad5ASM infection. Data are means ± SD from ≥4 independent experiments. **P* < 0.05.

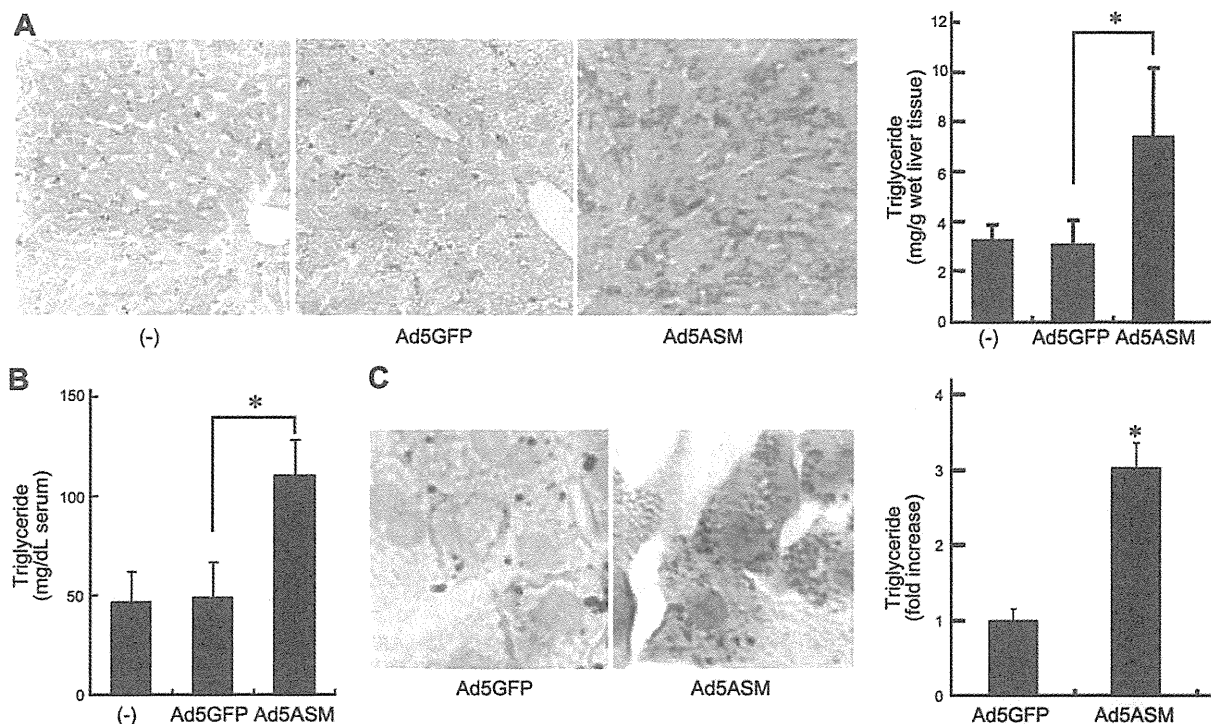


Figure 2. ASM stimulates lipid accumulation. *A*) Wild-type mice were infected with Ad5GFP or Ad5ASM (5×10^8 PFU/mouse). Hepatic lipid content was assessed by Oil Red O staining (left panel; original view $\times 200$) and triglyceride measurement (right panel) in food-deprived wild-type mice at 7 d after the adenovirus infection. *B*) Serum triglycerides were determined in food-deprived wild-type mice at 7 d after the infection. *C*) Primary cultured rat hepatocytes were infected with Ad5GFP or Ad5ASM (10 PFU/cell). Lipid droplets were assessed by Oil Red O staining (original view $\times 800$). Triglyceride level in hepatocytes was determined (right panel). Data are means \pm SD from ≥ 4 independent experiments. * $P < 0.05$.

metabolism in hepatocytes. On the basis of the fundamental roles of AKT in glucose and lipid metabolism, we investigated the role of AKT in ASM-mediated glucose, glycogen, and lipid metabolism. First, we examined whether ASM alters AKT signaling. Food intake stimulates AKT and GSK3 β phosphorylation in mouse liver (Fig. 3A). Introduction of exogenous ASM increased AKT activation under food-deprivation conditions and further increased under feeding conditions (Fig. 3A) without increasing serum insulin levels (data not shown) in comparison with control virus-infected animals. We further tested the requirement for insulin in ASM-induced AKT activation. In insulin-free conditions, introduction of ASM still increased AKT and GSK3 β phosphorylation in primary cultured rat hepatocytes (Fig. 3B, left panel). High-dose glucose did not affect AKT and GSK3 β phosphorylation in primary hepatocytes (Fig. 3B, left panel). These results suggest that ASM-induced AKT activation is not mediated by insulin or a response to increased intracellular glucose. In contrast, overexpression of DN-AKT abolished ASM-mediated AKT and GSK3 β activity (Fig. 3B, right panel). DN-AKT overexpression also abolished ASM-induced glycogen deposition and lipid accumulation (Fig. 3C, D). These results suggest that ASM regulates glucose, glycogen, and lipid metabolism *via* activation of AKT.

ASM decreases AMPK phosphorylation and increases GLUT2 expression in hepatocytes

Because AMPK is an important component in glucose metabolism, the effects of ASM on AMPK signaling were examined. Glycogen deposition induced by high-dose glucose was increased by DN-AMPK and reduced by CA-AMPK (Supplemental Fig. S2C, D) with no observed effects on AKT and GSK3 β phosphorylation (data not shown), indicating that AMPK activation reduced glycogen synthesis; this result is consistent with previous studies (3). Then, we assessed the role of AMPK in ASM-mediated effects. In the control virus-infected livers, food intake did not affect AMPK phosphorylation (Fig. 4A), consistent with a previous report (27). In contrast, introduction of ASM reduced AMPK phosphorylation in response to food intake (Fig. 4A). ASM also increased food intake-related GLUT2 protein expression in the liver (Fig. 4A). A previous study gave indirect evidence that high glycogen content represses AMPK activation in skeletal muscle (28). However, our data demonstrated that AMPK phosphorylation was reduced by ASM in primary cultured hepatocytes under normal glucose conditions (Fig. 4B), in which the glycogen content was lower than that in Ad5GFP-infected cells cultured in high-dose glucose medium (Fig. 1E). These results suggest that the AMPK inactivation by ASM is not mediated by a response to increased intracellular glycogen. In primary cultured hepatocytes,

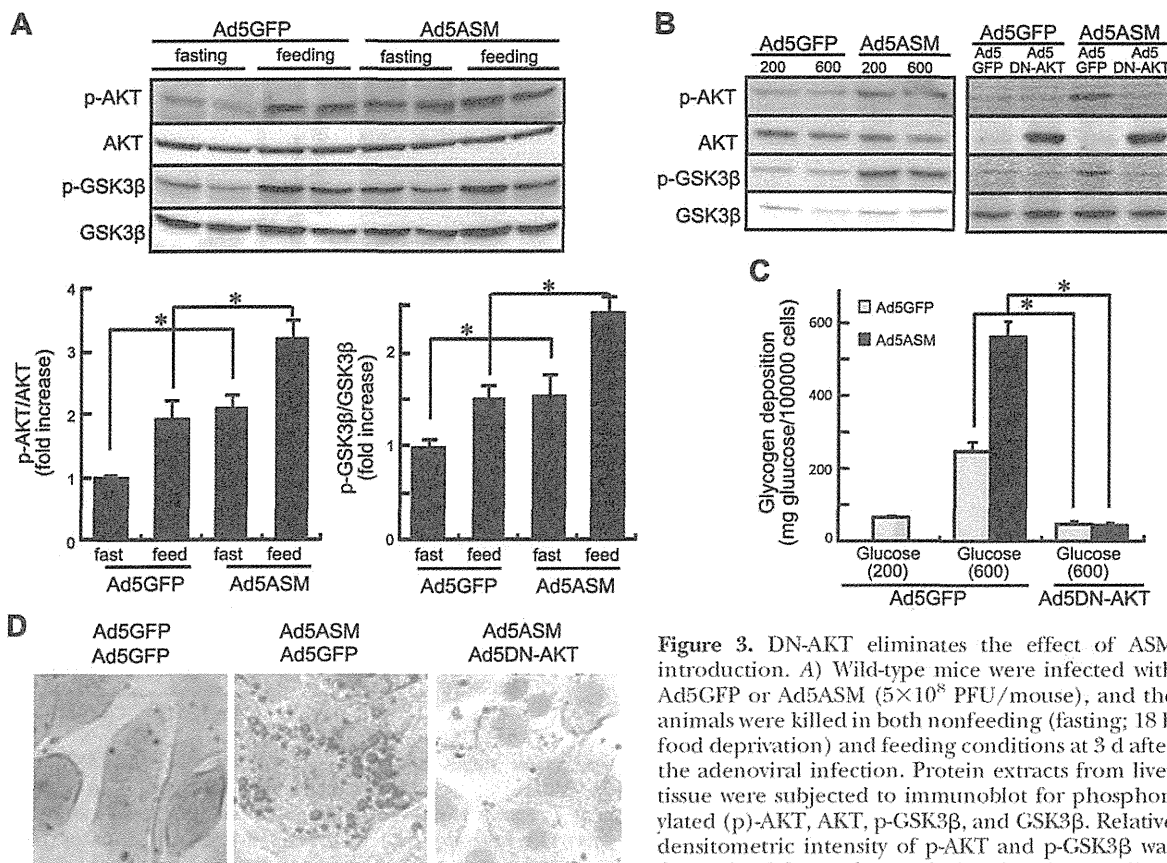


Figure 3. DN-AKT eliminates the effect of ASM introduction. *A*) Wild-type mice were infected with Ad5GFP or Ad5ASM (5×10^8 PFU/mouse), and the animals were killed in both nonfeeding (fasting; 18 h food deprivation) and feeding conditions at 3 d after the adenoviral infection. Protein extracts from liver tissue were subjected to immunoblot for phosphorylated (p)-AKT, AKT, p-GSK3 β , and GSK3 β . Relative densitometric intensity of p-AKT and p-GSK3 β was determined for each protein band and normalized

to AKT and GSK3 β , respectively (bottom panels). *B*) Primary cultured rat hepatocytes infected with Ad5GFP or Ad5ASM (10 PFU/cell) were further infected with Ad5GFP or Ad5DN-AKT or treated with or without high-dose glucose (600 mg/dl; normal glucose, 200 mg/dl) for 8 h. Protein extracts from hepatocytes were subjected to immunoblot for p-AKT, AKT, p-GSK3 β , and GSK3 β . *C*) Primary cultured rat hepatocytes infected with Ad5GFP or Ad5ASM plus Ad5GFP or Ad5DN-AKT were treated with or without high-dose glucose. Glycogen content was determined in hepatocytes at 8 h after the high-dose glucose treatment. *D*) Primary cultured rat hepatocytes were infected with Ad5GFP or Ad5ASM plus Ad5GFP or Ad5DN-AKT. Lipid droplets were assessed by Oil Red O staining in hepatocytes (original view $\times 800$). Results shown are representative of ≥ 3 independent experiments. Data are means \pm sd from ≥ 4 independent experiments. $*P < 0.05$.

high-dose glucose slightly reduced AMPK phosphorylation (Fig. 4*B*), as shown in a previous report in HepG2 hepatoblastoma cells (29), suggesting that the refractoriness of AMPK by food intake was probably due to systemic mediators. In addition to AMPK, GLUT2 protein and mRNA levels were increased in ASM-expressing primary hepatocytes (Fig. 4*B*, *C*). CA-AMPK partially inhibited glycogen deposition and lipid accumulation induced by ASM (Fig. 4*D*, *E*). These results suggest that reduced AMPK activation is also crucial for ASM-mediated glucose metabolism.

ASM activates AKT through the SphK/S1P pathway

ASM hydrolyzes sphingomyelin into ceramide, which is further hydrolyzed and phosphorylated by ceramidase and SphK to form S1P. Because S1P activates AKT in hepatocytes (20), we investigated the contribution of S1P generation to ASM-mediated glucose and lipid metabolism. The ASM-induced phosphorylation of

AKT and GSK3 β was reduced in SphK1 $^{-/-}$ hepatocytes (Fig. 5*A*). Of note, S1P formation was inhibited in SphK1 $^{-/-}$ cells (Fig. 5*B*, left panels). Overexpression of neutral ceramidase (NCD) or exogenous S1P activated AKT (Fig. 5*B*, middle and right panels) in hepatocytes, as we reported previously (20). These results suggest that S1P generated by the breakdown of sphingomyelin contributes to ASM-induced AKT activation. We then examined the involvement of S1PR. Hepatocytes were treated with PTX because S1PRs coupled with G $_i$ are sensitive to PTX. ASM-mediated AKT activation was reduced by PTX treatment (Fig. 5*C*), indicating that ASM generates S1P, which further activates AKT, at least partially *via* S1PRs. ASM-induced glycogen deposition and lipid accumulation were also reduced in SphK1 $^{-/-}$ hepatocytes (Fig. 6*A*, *B*), whereas the sphingomyelin and ceramide levels were similar to those in wild-type hepatocytes (data not shown). Moreover, SphK1 $^{-/-}$ mice did not show hepatic steatosis by exogenous ASM introduction (Fig. 6*C*). In contrast to

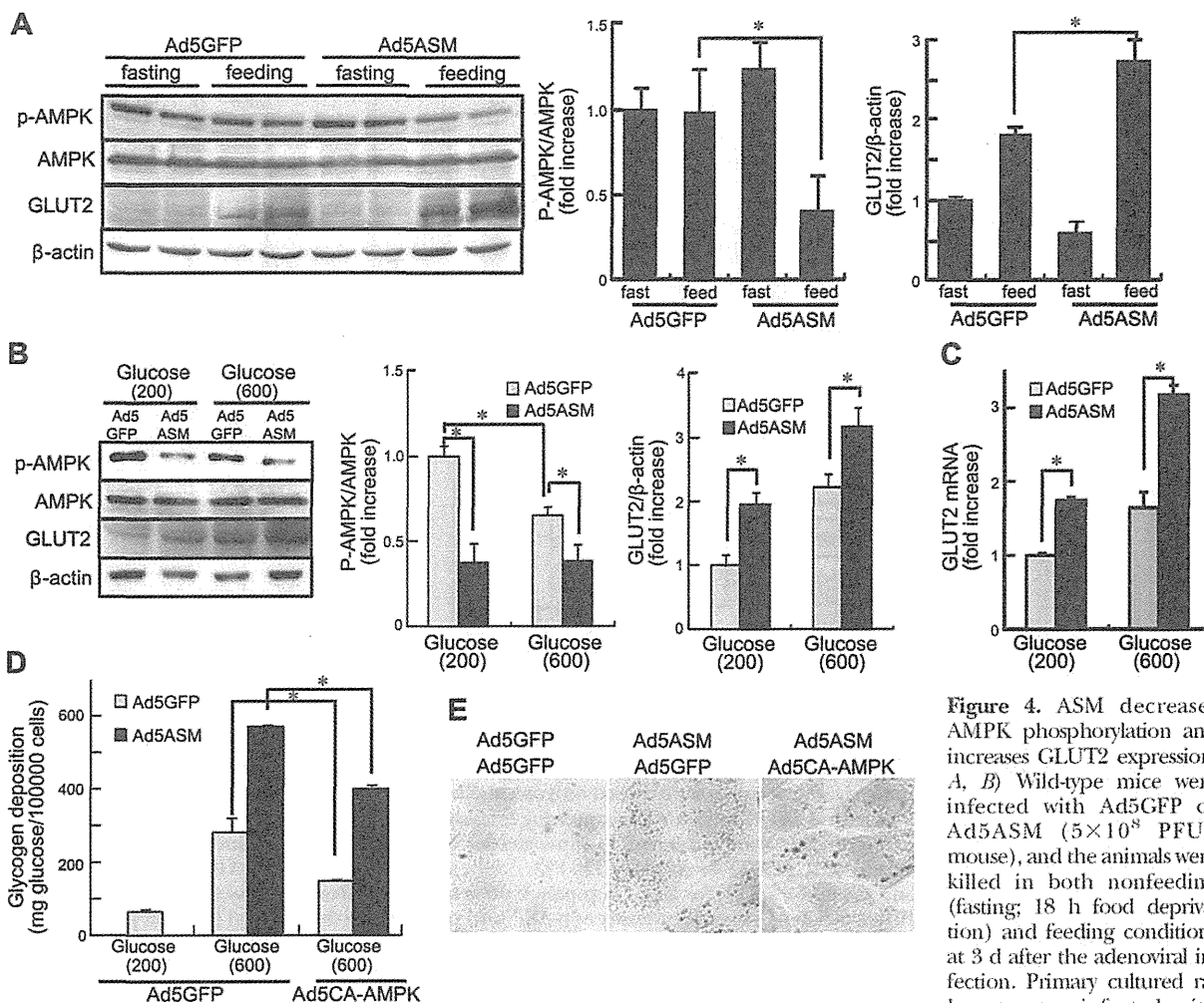


Figure 4. ASM decreases AMPK phosphorylation and increases GLUT2 expression. *A, B*) Wild-type mice were infected with Ad5GFP or Ad5ASM (5×10^8 PFU/mouse), and the animals were killed in both nonfeeding (fasting; 18 h food deprivation) and feeding conditions at 3 d after the adenoviral infection. Primary cultured rat hepatocytes infected with

Ad5GFP or Ad5ASM (10 PFU/cell) were cultured in normal (200 mg/dl) or high-dose glucose (600 mg/dl) conditions for 8 h. Left panels: protein extracts from the liver tissue (*A*) or the hepatocytes (*B*) were subjected to immunoblot for phosphorylated (p)-AMPK, AMPK, GLUT2, and β -actin. Right panels: relative densitometric intensity of p-AMPK and GLUT2 was determined for each protein band and normalized to AMPK and β -actin, respectively. *C*). mRNA levels of GLUT2 in hepatocytes were determined by quantitative real-time RT-PCR and normalized by 18S ribosomal RNA. *D*) Primary cultured rat hepatocytes infected with Ad5GFP or Ad5CA-AMPK were further infected with Ad5GFP or Ad5ASM. Cells were then incubated in normal or high-dose glucose conditions for 8 h. Glycogen content in hepatocytes was determined. *E*) Primary cultured rat hepatocytes were infected with Ad5GFP, Ad5CA-AMPK, and/or Ad5ASM. Lipid droplets in hepatocytes were assessed by Oil Red O staining (original view $\times 800$). Results shown are representative of ≥ 3 independent experiments. Data are means \pm SD from ≥ 4 independent experiments. $*P < 0.05$.

AKT, AMPK was not affected by S1P administration or NCD overexpression (Fig. 5*B*, middle panel). As in wild-type mice, SphK1^{-/-} mice expressing exogenous ASM showed decreased phosphorylation of AMPK (Fig. 5*A*), indicating that the SphK/S1P pathway is not required for ASM-induced AMPK down-regulation.

ASM deficiency inhibits glucose uptake, glycogen deposition, and lipid accumulation in hepatocytes

Finally, we tested whether ASM deficiency causes glucose intolerance. Sphingomyelin accumulation and ceramide reduction were observed in hepatocytes isolated from ASM^{-/-} mice (Supplemental Table S1). Blood glucose levels in ASM^{-/-} mice were higher than those in ASM^{+/+}

mice throughout the IPGTT period without any changes in insulin levels (Fig. 7). To further investigate the specific role of ASM in hepatocytes, primary hepatocytes were isolated and treated with high-dose glucose (600 mg/dl), which increased glycogen levels (Fig. 8*A*). Imipramine, a tricyclic antidepressant, causes proteolysis of the active 72-kDa ASM form, thus inhibiting ASM activity (30). Pretreatment with imipramine inhibited high-dose glucose-induced glycogen deposition (Fig. 8*A*), as did the knockout of ASM in mouse hepatocytes (Fig. 8*B*). Moreover, high-dose glucose increased lipid droplets in primary hepatocytes, and imipramine or ASM deficiency suppressed this effect (Fig. 8*C, D*). These results suggest that high-dose glucose increases glucose uptake, resulting in glycogen deposition and lipid accumulation in hepato-

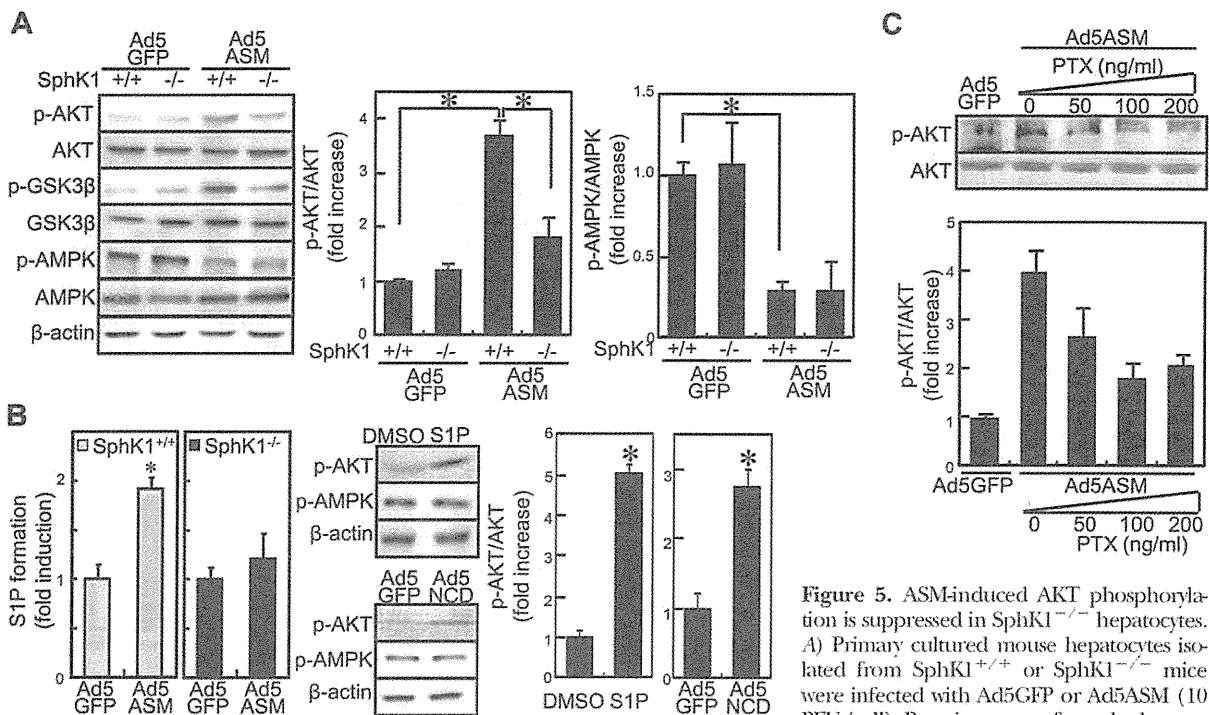


Figure 5. ASM-induced AKT phosphorylation is suppressed in SphK1^{-/-} hepatocytes. *A*) Primary cultured mouse hepatocytes isolated from SphK1^{+/+} or SphK1^{-/-} mice were infected with Ad5GFP or Ad5ASM (10 PFU/cell). Protein extracts from the hepatocytes were subjected to immunoblot for phosphorylated (p)-AKT, AKT, p-GSK3β, GSK3β, p-AMPK, AMPK, and β-actin. *B*) [³H]Serine-labeled hepatocytes from SphK1^{+/+} or SphK1^{-/-} mice were infected with Ad5GFP or Ad5ASM. Radiolabeled S1P was measured (left panels). Primary cultured rat hepatocytes were treated with or without S1P (1 μM) for 8 h (middle top panel). Primary cultured rat hepatocytes were infected with Ad5GFP or adenovirus expressing human neutral ceramidase (Ad5NCD) (middle bottom panel). Protein extracts from the hepatocytes were subjected to immunoblot for p-AKT, p-AMPK, and β-actin. *C*) Primary cultured rat hepatocytes were infected with Ad5GFP or Ad5ASM (10 PFU/cell), and incubated for 2 h. Then, cells were treated with or without the indicated concentration of PTX for 24 h. Top panel: protein extracts from hepatocytes were subjected to immunoblot for p-AKT and AKT. Relative densitometric intensity of p-AKT and p-AMPK was determined for each protein band of the sample and normalized to AKT and AMPK, respectively (*A*, *B*, right panels; *C*, bottom panel). Results shown are representative of ≥3 independent experiments. Data are means ± SD from ≥4 independent experiments. **P* < 0.05.

cytes. In contrast, ASM deficiency inhibits glucose uptake, glycogen deposition, and lipid accumulation, resulting in glucose intolerance. In ASM^{-/-} mice, similar levels of GSK3β phosphorylation were induced by food intake, whereas GLUT2 induction was reduced in comparison to

the livers of ASM^{+/+} mice (Fig. 9A). Reduction of AMPK phosphorylation and induction of GLUT2 by high-dose glucose were inhibited in ASM^{-/-} hepatocytes (Fig. 9B), whereas high-dose glucose did not affect AKT phosphorylation (data not shown). These results suggest that glu-

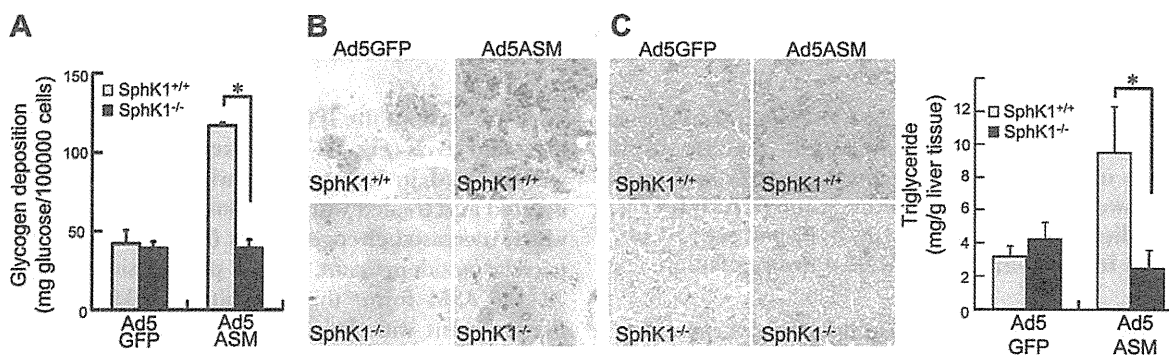


Figure 6. ASM-induced glycogen deposition and lipid accumulation are suppressed in SphK1^{-/-} hepatocytes. *A*) Primary cultured hepatocytes isolated from SphK1^{+/+} or SphK1^{-/-} mice were infected with Ad5GFP or Ad5ASM. Glycogen content in hepatocytes was determined. *B*) Lipid droplets in SphK1^{+/+} or SphK1^{-/-} hepatocytes infected with Ad5GFP or Ad5ASM were assessed by Oil Red O staining (original view ×800). *C*) SphK1^{+/+} or SphK1^{-/-} mice were infected with Ad5GFP or Ad5ASM, followed by assessment for hepatic lipid content by Oil Red O staining (left panel; original view ×200) and triglyceride measurement (right panel) in food-deprivation conditions at 7 d after the infection (original view ×200). Results shown are representative of ≥3 independent experiments. Data are means ± SD from ≥4 independent experiments. **P* < 0.05.

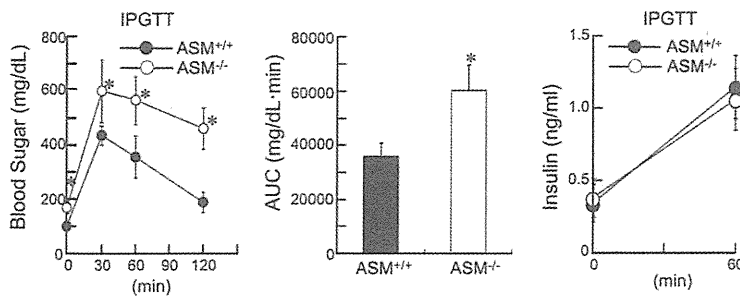


Figure 7. ASM^{-/-} mice were glucose intolerant. A) ASM^{+/+} and ASM^{-/-} mice were deprived of food for 18 h, and IPGTT was performed by administering a glucose load of 2 mg/g body weight. Serial glucose (left panel) and insulin (right panel) were measured at the indicated time points. Blood glucose values for area under the curve (AUC) were calculated (middle panel). Results shown are representative of ≥ 3 independent experiments. Data are means \pm sd from ≥ 4 independent experiments. * $P < 0.05$.

glucose intolerance in ASM^{-/-} mice was due, at least in part, to insufficient reduction of AMPK activity and induction of GLUT2.

DISCUSSION

The present study addresses the contributions of ASM to glucose and lipid metabolism in the liver. The sphingomyelin/ceramide/S1P pathway is involved in glucose metabolism (6–9, 12–14, 21). Food intake reduced most sphingomyelin species in the mouse liver (Supplemental Table S2). Likewise, high-dose glucose reduced sphingomyelin species in primary cultured hepatocytes (Supplemental Table S2), suggesting that this pathway is related to glucose metabolism in hepatocytes. In our study using hepatocytes, ASM induced insulin-like effects such as glucose uptake, glycogen deposition, and lipid accumulation *via* S1P-mediated

AKT activation. Ceramide attenuates insulin signaling, including AKT activation (14–16), thereby contributing to insulin resistance through multiple pathways (13, 15). In primary cultured hepatocytes, the effect of ASM introduction on ceramide level was smaller than that in sphingomyelin degradation, suggesting that the generated ceramide is further converted to S1P. Ceramide and S1P often exert opposing effects; thus, the balance between these two sphingolipids may be important for AKT activation. During ASM activation, the balance is inclined toward S1P, resulting in AKT activation. Indeed, ASM did not activate AKT in SphK1^{-/-} hepatocytes, suggesting that ASM mediates insulin-like effects *via* S1P formation. S1P acts as a ligand for the S1PRs and also as an intracellular second messenger (31, 32). Among S1PRs, G_i-associated S1PR1 (33) is mainly expressed in the liver (34), and PTX pretreatment inhibited exogenous S1P-induced AKT phosphorylation in

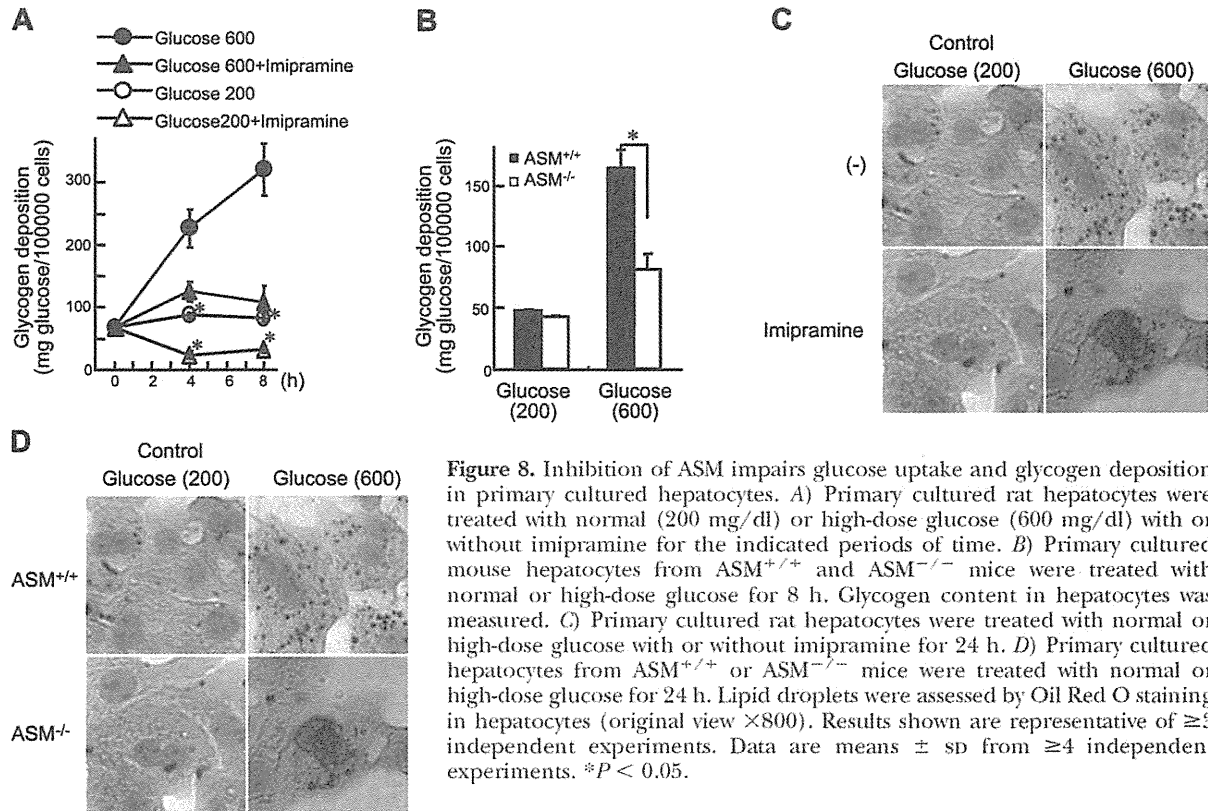


Figure 8. Inhibition of ASM impairs glucose uptake and glycogen deposition in primary cultured hepatocytes. A) Primary cultured rat hepatocytes were treated with normal (200 mg/dl) or high-dose glucose (600 mg/dl) with or without imipramine for the indicated periods of time. B) Primary cultured mouse hepatocytes from ASM^{+/+} and ASM^{-/-} mice were treated with normal or high-dose glucose for 8 h. Glycogen content in hepatocytes was measured. C) Primary cultured rat hepatocytes were treated with normal or high-dose glucose with or without imipramine for 24 h. D) Primary cultured hepatocytes from ASM^{+/+} or ASM^{-/-} mice were treated with normal or high-dose glucose for 24 h. Lipid droplets were assessed by Oil Red O staining in hepatocytes (original view $\times 800$). Results shown are representative of ≥ 3 independent experiments. Data are means \pm sd from ≥ 4 independent experiments. * $P < 0.05$.

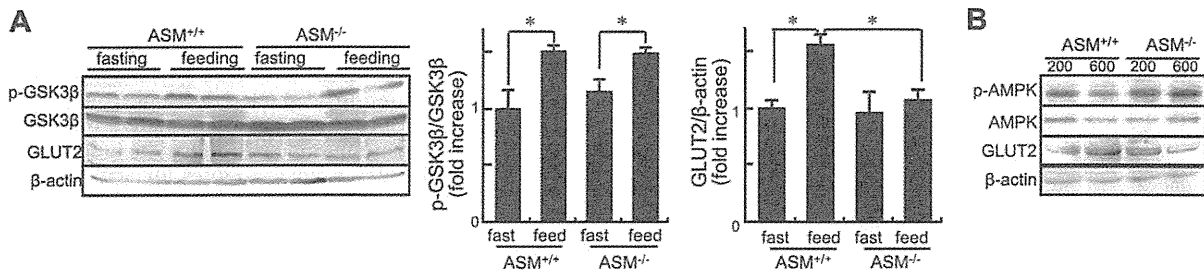


Figure 9. Inhibition of ASM suppresses GLUT2 induction. A) $ASM^{+/+}$ and $ASM^{-/-}$ mice were killed in both nonfeeding (fasting; 18 h food deprivation) and feeding conditions. Protein extracts from liver tissue were subjected to immunoblot for phosphorylated (p)-GSK3 β , GSK3 β , GLUT2, and β -actin (left panel). Relative densitometric intensity of p-GSK3 β (middle panel) and GLUT2 (right panel) was determined for each protein band of the liver tissue sample and normalized to GSK3 β and β -actin, respectively. B) Primary cultured hepatocytes from $ASM^{+/+}$ and $ASM^{-/-}$ mice were treated with normal (200 mg/dl) or high-dose glucose (600 mg/dl) for 8 h. Protein extracts from hepatocytes were subjected to immunoblot for p-AMPK, AMPK, GLUT2, and β -actin. Results shown are representative of ≥ 3 independent experiments. * $P < 0.05$.

primary cultured hepatocytes (data not shown), suggesting that S1P may activate AKT through predominantly S1PR1. PTX treatment partially inhibits ASM-induced AKT activation, suggesting that the generated S1P activates AKT at least partially *via* S1PRs and may also activate AKT through receptor-independent mechanisms.

In addition to AKT, AMPK also contributes to glucose metabolism. AMPK is a serine/threonine protein kinase that senses the immediate availability of cellular energy. Activated AMPK switches on catabolic pathways and switches off protein, carbohydrate, and lipid biosynthesis (anabolic pathways; ref. 35). Activation of AMPK in the liver reduces glycogen synthesis and lipogenesis as well as expression of GLUT2 (3). Activation of AMPK by 5-amino-4-imidazolecarboxamide riboside diminishes GLUT2 expression in primary cultured hepatocytes (36). Indeed, DN-AMPK increased glycogen deposition and lipid accumulation in primary hepatocytes and HepG2 cells (data not shown and ref. 37). Thus, in addition to increased AKT activation, reduced AMPK activity may be associated with another anabolic effect of ASM. Ceramide decreases (38) but S1P increases (39) AMPK phosphorylation in endothelial cells. In our study, ASM-induced AMPK inhibition in hepatocytes was independent of S1P. Thus, the decrease in AMPK activity may be due to ceramide processed by ASM.

Ad5ASM-infected mice showed improved glucose tolerance. Because adenovirus preferentially infects hepatocytes, the decrease in blood glucose was due to a variation of hepatic glucose metabolism, although sphingolipids have roles in glucose metabolism in muscle (40) and adipocytes (6–8). The ASM-induced decrease in blood glucose may be attributed to increased uptake of hepatic glucose rather than decreased production, because introduction of ASM did not affect the activity of adenylate cyclase, the glucagon target enzyme, in primary cultured rat hepatocytes (data not shown). The effects of ASM on hepatocytes are comparable to those of insulin. However, the introduction of hepatic ASM improved hyperglycemia in *db/db* mice with type 2 diabetes without increasing insulin levels (data not

shown), indicating that ASM may reduce blood glucose regardless of the presence of insulin resistance. Instead of decreasing blood glucose, ASM increased hepatic triglyceride content, suggesting that ASM stimulates lipogenesis, in which transported glucose is converted to triacylglycerol (41). The effects of exogenous ASM in the liver are similar to the effects of deletion of hepatic phosphatase and tension homolog on chromosome 10 (PTEN), which is a negative regulator of AKT. Deletion of PTEN in the liver results in hyperphosphorylation of hepatic AKT and improves glucose tolerance but induces fatty liver in mice (42).

$ASM^{-/-}$ mice are glucose intolerant. The abnormality is not due to inactivation of the AKT/GSK3 β pathway but is due, in part, to insufficient reduction of AMPK activity and induction of GLUT2. In addition, crosstalk may occur between ASM and various signaling pathways, including those of glucose and lipid metabolism, because ASM regulates sphingolipids in lipid raft microdomains that function as platforms for signal transduction and protein sorting (18). For example, disruption of lipid raft microdomains or chronic ethanol exposure inhibits localization of TC10 to lipid rafts,

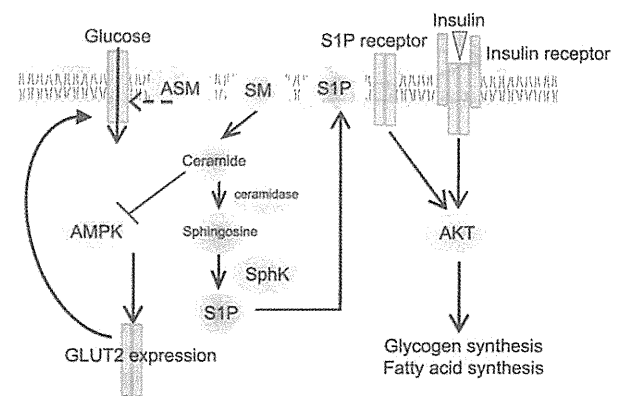



Figure 10. Hypothetical signals induced by ASM. Acid sphingomyelinase regulates glucose and lipid metabolism through AKT activation and AMPK suppression in hepatocytes. AKT activation is induced through S1P formation. AMPK suppression increases GLUT2 expression.

which induces GLUT4 translocation and glucose intake without affecting phosphatidylinositol-3 kinase/AKT signaling in adipocytes (43, 44). Pretreatment with imipramine inhibited high-dose glucose-induced lipid accumulation in rat hepatocytes, as did the knockout of ASM in mouse hepatocytes. As reported previously, the ASM inhibitor desipramine attenuates triglyceride increase by high-dose palmitic acid treatment in HepG2 cells (9). Moreover, a high-fat, high-cholesterol diet does not induce hepatic triacylglyceride accumulation in ASM^{-/-} mice under LDL receptor-deficient conditions (9). These observations further support the role of ASM as a regulator of triglyceride synthesis in addition to glucose uptake. Further studies will determine the precise mechanism underlying the anabolic effects of ASM and its activation and ceramide/S1P regulation (45). The hypothetical roles of ASM are schematically summarized in Fig. 10.

In conclusion, overexpression of ASM in the liver improves glucose tolerance in both wild-type and diabetic *db/db* mice. ASM stimulates glucose uptake, glycogen deposition, and lipid accumulation in hepatocytes via AKT and GSK3 β phosphorylation, which requires S1P formation. In addition, ASM decreases AMPK phosphorylation through ceramides, leading to GLUT2 up-regulation. Indeed, inactivation of ASM produces glucose intolerance in hepatocytes. Targeting ASM may become a new therapeutic strategy in type 2 diabetes. 

The authors thank Dr. Jacek Bielawski (Medical University of South Carolina, Charleston, SC, USA) for sphingolipid measurement, Dr. Yoko Sugiyama (Gifu University Graduate School of Medicine, Gifu, Japan) for measurement of adenylate cyclase activity, and Dr. Kenneth Walsh (Boston University, Boston, MA, USA) for adenoviruses encoding CA-AMPK and DN-AMPK. This work was supported by grants from Mitsubishi Pharma Research Foundation and the Ministry of Education, Culture, Sports, Science, and Technology of Japan (19790478 and 21790657 to Y.O. and 21390179 to M.S.).

REFERENCES

- Thorens, B., Sarkar, H. K., Kaback, H. R., and Lodish, H. F. (1988) Cloning and functional expression in bacteria of a novel glucose transporter present in liver, intestine, kidney, and β -pancreatic islet cells. *Cell* **55**, 281–290
- Rencurel, F., Waeber, G., Antoine, B., Rocchiccioli, F., Maulard, P., Girard, J., and Leturque, A. (1996) Requirement of glucose metabolism for regulation of glucose transporter type 2 (GLUT2) gene expression in liver. *Biochem. J.* **314**(Pt. 3), 903–909
- Foretz, M., Ancellin, N., Andreelli, F., Saintillan, Y., Grondin, P., Kahn, A., Thorens, B., Vaulont, S., and Viollet, B. (2005) Short-term overexpression of a constitutively active form of AMP-activated protein kinase in the liver leads to mild hypoglycemia and fatty liver. *Diabetes* **54**, 1331–1339
- Smith, E. L., and Schuchman, E. H. (2008) The unexpected role of acid sphingomyelinase in cell death and the pathophysiology of common diseases. *FASEB J.* **22**, 3419–3431
- Gorska, M., Baranczuk, E., and Dobrzyn, A. (2003) Secretory Zn²⁺-dependent sphingomyelinase activity in the serum of patients with type 2 diabetes is elevated. *Horm. Metab. Res.* **35**, 506–507
- Liu, P., Leffler, B. J., Weeks, L. K., Chen, G., Bouchard, C. M., Strawbridge, A. B., and Elmendorf, J. S. (2004) Sphingomyelinase activates GLUT4 translocation via a cholesterol-dependent mechanism. *Am. J. Physiol. Cell Physiol.* **286**, C317–C329
- David, T. S., Ortíz, P. A., Smith, T. R., and Turinsky, J. (1998) Sphingomyelinase has an insulin-like effect on glucose transporter translocation in adipocytes. *Am. J. Physiol.* **274**, R1446–1453
- Al-Makdissy, N., Younsi, M., Pierre, S., Ziegler, O., and Donner, M. (2003) Sphingomyelin/cholesterol ratio: an important determinant of glucose transport mediated by GLUT-1 in 3T3-L1 preadipocytes. *Cell. Signal.* **15**, 1019–1030
- Deevska, G. M., Rozenova, K. A., Giltiay, N. V., Chambers, M. A., White, J., Boyanovsky, B. B., Wei, J., Daugherty, A., Smart, E. J., Reid, M. B., Merrill, A. H., Jr., and Nikolova-Karakashian, M. (2009) Acid sphingomyelinase deficiency prevents diet-induced hepatic triacylglycerol accumulation and hyperglycemia in mice. *J. Biol. Chem.* **284**, 8359–8368
- Jenkins, R. W., Canals, D., and Hannun, Y. A. (2009) Roles and regulation of secretory and lysosomal acid sphingomyelinase. *Cell. Signal.* **21**, 836–846
- Hannun, Y. A. (1996) Functions of ceramide in coordinating cellular responses to stress. *Science* **274**, 1855–1859
- Summers, S. A., and Nelson, D. H. (2005) A role for sphingolipids in producing the common features of type 2 diabetes, metabolic syndrome X, and Cushing's syndrome. *Diabetes* **54**, 591–602
- Holland, W. L., Brozinick, J. T., Wang, L. P., Hawkins, E. D., Sargent, K. M., Liu, Y., Narra, K., Hoehn, K. L., Knotts, T. A., Siesky, A., Nelson, D. H., Karathanasis, S. K., Fontenot, G. K., Birnbaum, M. J., and Summers, S. A. (2007) Inhibition of ceramide synthesis ameliorates glucocorticoid-, saturated-fat-, and obesity-induced insulin resistance. *Cell Metab.* **5**, 167–179
- Holland, W. L., and Summers, S. A. (2008) Sphingolipids, insulin resistance, and metabolic disease: new insights from in vivo manipulation of sphingolipid metabolism. *Endocr. Rev.* **29**, 381–402
- Wymann, M. P., and Schneider, R. (2008) Lipid signalling in disease. *Nat. Rev. Mol. Cell Biol.* **9**, 162–176
- Stratford, S., DeWald, D. B., and Summers, S. A. (2001) Ceramide dissociates 3'-phosphoinositide production from pleckstrin homology domain translocation. *Biochem. J.* **354**, 359–368
- Liangpumsakul, S., Sozio, M. S., Shin, E., Zhao, Z., Xu, Y., Ross, R. A., Zeng, Y., and Crabb, D. W. Inhibitory effect of ethanol on AMPK phosphorylation is mediated in part through elevated ceramide levels. *Am. J. Physiol. Gastrointest. Liver Physiol.* **298**, G1004–G1012
- Tani, M., Ito, M., and Igarashi, Y. (2007) Ceramide/sphingosine/sphingosine 1-phosphate metabolism on the cell surface and in the extracellular space. *Cell. Signal.* **19**, 229–237
- Osawa, Y., Banno, Y., Nagaki, M., Brenner, D. A., Naiki, T., Nozawa, Y., Nakashima, S., and Moriwaki, H. (2001) TNF α -induced sphingosine 1-phosphate inhibits apoptosis through a phosphatidylinositol 3-kinase/Akt pathway in human hepatocytes. *J. Immunol.* **167**, 173–180
- Osawa, Y., Uchinami, H., Bielawski, J., Schwabe, R. F., Hannun, Y. A., and Brenner, D. A. (2005) Roles for C16-ceramide and sphingosine 1-phosphate in regulating hepatocyte apoptosis in response to tumor necrosis factor- α . *J. Biol. Chem.* **280**, 27879–27887
- Rapizzi, E., Taddei, M. L., Fiaschi, T., Donati, C., Bruni, P., and Chiarugi, P. (2009) Sphingosine 1-phosphate increases glucose uptake through trans-activation of insulin receptor. *Cell. Mol. Life Sci.* **66**, 3207–3218
- Osawa, Y., Hannun, Y. A., Proia, R. L., and Brenner, D. A. (2005) Roles of AKT and sphingosine kinase in the antiapoptotic effects of bile duct ligation in mouse liver. *Hepatology* **42**, 1320–1328
- Allende, M. L., Sasaki, T., Kawai, H., Olivera, A., Mi, Y., van Echten-Deckert, G., Hajdu, R., Rosenbach, M., Keohane, C. A., Mandala, S., Spiegel, S., and Proia, R. L. (2004) Mice deficient in sphingosine kinase 1 are rendered lymphopenic by FTY720. *J. Biol. Chem.* **279**, 52487–52492
- Adachi, M., and Brenner, D. A. (2008) High molecular weight adiponectin inhibits proliferation of hepatic stellate cells via activation of adenosine monophosphate-activated protein kinase. *Hepatology* **47**, 677–685

25. Bligh, E.G., and Dyer, W. J. (1959) A rapid method of total lipid extraction and purification. *Can. J. Biochem. Physiol.* **37**, 911–917
26. Pettus, B. J., Bielawski, J., Porcelli, A. M., Reames, D. L., Johnson, K. R., Morrow, J., Chalfant, C. E., Obeid, L. M., and Hannun, Y. A. (2003) The sphingosine kinase 1/sphingosine-1-phosphate pathway mediates COX-2 induction and PGE₂ production in response to TNF- α . *FASEB J.* **17**, 1411–1421
27. Gonzalez, A. A., Kumar, R., Mulligan, J. D., Davis, A. J., Weindruch, R., and Saupé, K. W. (2004) Metabolic adaptations to fasting and chronic caloric restriction in heart, muscle, and liver do not include changes in AMPK activity. *Am. J. Physiol. Endocrinol. Metab.* **287**, E1032–E1037
28. Wojtaszewski, J. F., Jorgensen, S. B., Hellsten, Y., Hardie, D. G., and Richter, E. A. (2002) Glycogen-dependent effects of 5-aminoimidazole-4-carboxamide (AICA)-riboside on AMP-activated protein kinase and glycogen synthase activities in rat skeletal muscle. *Diabetes* **51**, 284–292
29. Zang, M., Zuccollo, A., Hou, X., Nagata, D., Walsh, K., Herscovitz, H., Brecher, P., Ruderman, N. B., and Cohen, R. A. (2004) AMP-activated protein kinase is required for the lipid-lowering effect of metformin in insulin-resistant human HepG2 cells. *J. Biol. Chem.* **279**, 47898–47905
30. Grassme, H., Gulbins, E., Brenner, B., Ferlinz, K., Sandhoff, K., Harzer, K., Lang, F., and Meyer, T. F. (1997) Acidic sphingomyelinase mediates entry of *N. gonorrhoeae* into nonphagocytic cells. *Cell* **91**, 605–615
31. Pyne, S., and Pyne, N. J. (2002) Sphingosine 1-phosphate signalling and termination at lipid phosphate receptors. *Biochim. Biophys. Acta* **1582**, 121–131
32. Olivera, A., and Spiegel, S. (1993) Sphingosine-1-phosphate as second messenger in cell proliferation induced by PDGF and FCS mitogens. *Nature* **365**, 557–560
33. Siehler, S., and Manning, D. R. (2002) Pathways of transduction engaged by sphingosine 1-phosphate through G protein-coupled receptors. *Biochim. Biophys. Acta* **1582**, 94–99
34. Yang, A. H., Ishii, I., and Chun, J. (2002) In vivo roles of lysophospholipid receptors revealed by gene targeting studies in mice. *Biochim. Biophys. Acta* **1582**, 197–203
35. Hardie, D. G. (2007) AMP-activated/SNF1 protein kinases: conserved guardians of cellular energy. *Nat. Rev. Mol. Cell Biol.* **8**, 774–785
36. Leclerc, I., Lenzner, C., Gourdon, L., Vaulont, S., Kahn, A., and Viollet, B. (2001) Hepatocyte nuclear factor-4 α involved in type 1 maturity-onset diabetes of the young is a novel target of AMP-activated protein kinase. *Diabetes* **50**, 1515–1521
37. Hou, X., Xu, S., Maitland-Toolan, K. A., Sato, K., Jiang, B., Ido, Y., Lan, F., Walsh, K., Wierzbicki, M., Verbeuren, T. J., Cohen, R. A., and Zang, M. (2008) SIRT1 regulates hepatocyte lipid metabolism through activating AMP-activated protein kinase. *J. Biol. Chem.* **283**, 20015–20026
38. Wu, Y., Song, P., Xu, J., Zhang, M., and Zou, M. H. (2007) Activation of protein phosphatase 2A by palmitate inhibits AMP-activated protein kinase. *J. Biol. Chem.* **282**, 9777–9788
39. Igarashi, J., Shoji, K., Hashimoto, T., Moriue, T., Yoneda, K., Takamura, T., Yamashita, T., Kubota, Y., and Kosaka, H. (2009) Transforming growth factor- β 1 down-regulates caveolin-1 expression and enhances sphingosine 1-phosphate signaling in cultured vascular endothelial cells. *Am. J. Physiol. Cell Physiol.* **297**, C1263–C1274
40. Adams, J. M., 2nd, Pratipanawat, T., Berria, R., Wang, E., DeFronzo, R. A., Sullards, M. C., and Mandarino, L. J. (2004) Ceramide content is increased in skeletal muscle from obese insulin-resistant humans. *Diabetes* **53**, 25–31
41. Glimcher, L. H., and Lee, A. H. (2009) From sugar to fat: How the transcription factor XBP1 regulates hepatic lipogenesis. *Ann. N. Y. Acad. Sci.* **1173**(Suppl. 1), E2–E9
42. Stiles, B., Wang, Y., Stahl, A., Bassilian, S., Lee, W. P., Kim, Y.-J., Sherwin, R., Devaskar, S., Lesche, R., Magnuson, M. A., and Wu, H. (2004) Liver-specific deletion of negative regulator Pten results in fatty liver and insulin hypersensitivity. *Proc. Natl. Acad. Sci. U. S. A.* **101**, 2082–2087
43. Watson, R. T., Shigematsu, S., Chiang, S. H., Mora, S., Kanzaki, M., Macara, I. G., Saliel, A. R., and Pessin, J. E. (2001) Lipid raft microdomain compartmentalization of TC10 is required for insulin signaling and GLUT4 translocation. *J. Cell Biol.* **154**, 829–840
44. Sebastian, B. M., and Nagy, L. E. (2005) Decreased insulin-dependent glucose transport by chronic ethanol feeding is associated with dysregulation of the Cbl/TC10 pathway in rat adipocytes. *Am. J. Physiol. Endocrinol. Metab.* **289**, E1077–E1084
45. Zeidan, Y. H., and Hannun, Y. A. (2010) The acid sphingomyelinase/ceramide pathway: biomedical significance and mechanisms of regulation. *Curr. Mol. Med.* **10**, 454–466

Received for publication July 23, 2010.
Accepted for publication December 2, 2010.

Increased levels of serum leptin are a risk factor for the recurrence of stage I/II hepatocellular carcinoma after curative treatment

Naoki Watanabe, Koji Takai, Kenji Imai, Masahito Shimizu, Takafumi Naiki, Masahito Nagaki and Hisataka Moriwaki*

Department of Medicine, Gifu University Graduate School of Medicine, 1-1 Yanagido, Gifu 501-1194, Japan

(Received 15 December, 2010; Accepted 27 December, 2010; Published online 29 October, 2011)

Obesity and related adipocytokine disbalance increase the risk of hepatocellular carcinoma. To determine the impact of increased levels of leptin, an obesity-related adipocytokine, on the recurrence of hepatocellular carcinoma, we conducted a prospective case-series analysis. Eighty-five consecutive primary hepatocellular carcinoma patients at our hospital from January 2006 to December 2008 were analyzed. Serum leptin level significantly correlated with Body Mass Index, total body fat, and the amount of subcutaneous fat. They included 33 with stage I/II, who underwent curative treatment. The factors contributing to recurrence of hepatocellular carcinoma, including leptin, were subjected to univariate and multivariate analyses using the Cox proportional hazards model. Body Mass Index ($p = 0.0062$), total body fat ($p = 0.0404$), albumin ($p = 0.0210$), α -fetoprotein ($p = 0.0365$), and leptin ($p = 0.0003$) were significantly associated with the recurrence of hepatocellular carcinoma in univariate analysis. Multivariate analysis suggested that leptin (hazard ratio 1.25, 95% CI 1.07–1.49, $p = 0.0035$) was a sole independent predictor. Kaplan-Meier analysis showed that recurrence-free survival was lower in patients with greater serum leptin concentrations (>5 ng/mL, $p = 0.0221$). These results suggest that the serum leptin level is a useful biomarker for predicting the early recurrence of hepatocellular carcinoma.

Key Words: hepatocellular carcinoma, carcinogenesis, leptin, obesity, insulin resistance

Hepatocellular carcinoma (HCC) is the fifth most common malignancy worldwide and is estimated to cause approximately 500,000 deaths annually.⁽¹⁾ HCC frequently develops and in many cases recurs in cirrhotic livers due to persistent hepatitis B virus (HBV) and hepatitis C virus (HCV) infection; this is strongly associated with poor prognosis for this particular malignancy.⁽²⁾ Therefore, careful surveillance of high-risk groups for HCC is important to improve prognosis. Hence, there is a critical need to identify useful risk factors for the development of HCC. Infection with HBV and HCV, alcohol consumption, aflatoxin exposure, and immune-related hepatitis are accepted as significant risk factors for the development of primary HCC.⁽³⁾ Male gender, the presence of cirrhosis, high α -fetoprotein (AFP), large tumor foci, multiplicity of tumors, pathologically high-grade atypia of tumor cells, and the presence of portal venous invasion of tumors also raise the risk for HCC recurrence.^(4–8)

In addition to these factors, recent studies demonstrate that obesity⁽⁹⁾ and related metabolic abnormalities—especially diabetes mellitus (DM) and insulin resistance^(10,11)—are important risk factors for the development of HCC. For instance, insulin resistance significantly raises the risk of the recurrence of stage I HCC after curative treatment.⁽¹⁰⁾ Several pathophysiological mecha-

nisms linking obesity and HCC development have been proposed and include the emergence of insulin resistance and a state of chronic inflammation.^(12,13) Adipocytokine disbalance might also be involved in obesity-related liver carcinogenesis.⁽¹⁴⁾ Among the adipocytokines, it is well known that the serum levels of leptin, which regulate the homeostasis of glucose and lipid metabolism,⁽¹⁵⁾ are elevated in obese individuals.⁽¹⁶⁾ In addition, both *in vitro* and *in vivo* studies indicate that leptin might play a role in the development of several types of human malignancies, including HCC.^(17–21) These findings suggest that the dysregulation of serum leptin levels may be a critical link between obesity and liver carcinogenesis. However, whether leptin is a significant biomarker for predicting the development and/or recurrence of HCC has not been explored.

In this study, we measured the serum leptin concentration in patients with HCC and examined whether it is correlated with obesity and insulin resistance. In addition, we designed a prospective case-series analysis to examine the recurrence-free survival in consecutive patients with stage I/II HCC, who received curative treatment by surgical resection or radiofrequency ablation (RFA), stratified by serum leptin concentrations.

Materials and Methods

Patients. From January 2006 to December 2008, 85 primary HCC patients underwent initial treatment at our hospital. We measured visceral and subcutaneous fat volume using computed tomography (CT) scans at the umbilical level according to a previously reported technique (fatAnalyses and EV Insite R, PSP Corporation, Tokyo, Japan).⁽²²⁾ Tumor stage was defined according to the staging system of the Liver Cancer Study Group of Japan (LCSGJ).⁽²³⁾ HCC nodules were detected by imaging modalities including abdominal ultrasonography (US), dynamic CT, dynamic magnetic resonance imaging (MRI), and abdominal arteriography. The diagnosis of HCC was made from a typical hypervascular tumor stain on angiography and a typical dynamic-study finding of enhanced staining in the early phase and attenuation in the delayed phase.

Treatment, follow-up, and determination of recurrence. Fifteen patients were treated with surgical resection, 41 with RFA, 19 with transarterial chemoembolization (TACE), and 10 with transarterial infusion (TAI). Among them, we selected 33 curative cases that met the following criteria: tumor stage classified as I or II; and surgical resection or RFA conducted for the initial HCC treatment. In all 33 cases, therapeutic effects were judged to be

*To whom correspondence should be addressed.
E-mail: hmori@gifu-u.ac.jp

Table 1. Baseline demographic and clinical characteristics

Variable	Total patients (n = 85)
Sex (male/female)	54/31
Age (years)	73 [36–87]
BMI (kg/m ²)	23.2 [17.5–30.7]
Total body fat (cm ²)	188.81 [12.93–501.8]
Amount of visceral fat (cm ²)	76.43 [3.82–359.83]
Amount of subcutaneous fat (cm ²)	105.66 [9.11–265.26]
Etiology (B/C/B + C/other)*	8/55/2/20
Child-Pugh classification (A/B/C)	60/23/2
Ascites on CT imaging (present/absent)	7/78
ALB (g/dL)	3.5 [2.2–4.5]
PLT ($\times 10^4/\mu\text{L}$)	11.7 [3.0–76.4]
FPG (mg/dL)	97 [67–271]
FIRI ($\mu\text{U/mL}$)	8.115 [1.21–90.2]
HOMA-IR	2.245 [0.27–28.28]
HbA _{1c} (%)	5.3 [3.7–10.3]
Leptin (ng/mL)	5.0 [1.4–26.6]
Stage (I/II/III/IVA/IVB)	19/26/27/10/3
Initial treatment for HCC (resection/RFA/TACE/TAI)	15/41/19/10
AFP (ng/mL)	48 [0–222000]
PIVKA-II (mAU/mL)	170 [7–474000]
Follow-up period (days)	484 [14–1429]

Values are median [range]. *B means positive for hepatitis B surface antigen and C means positive for hepatitis C virus antibody. AFP, α -fetoprotein; B, hepatitis B virus; BMI, body mass index; C, hepatitis C virus; FPG, fasting plasma glucose; FIRI, fasting immunoreactive insulin; HbA_{1c}, hemoglobin A_{1c}; HCC, hepatocellular carcinoma; HOMA-IR, homeostasis model assessment of insulin resistance; PIVKA-II, protein induced by vitamin K absence or antagonists-II; RFA, radio-frequency ablation; TACE, transarterial chemoembolization; TAI, transarterial infusion.

curative using dynamic CT or MRI exhibiting a complete disappearance of the imaging characteristics of HCC described above.

Patients were thereafter followed up on a monthly outpatient basis using serum tumor markers every month, such as AFP and proteins induced by vitamin K absence or antagonists-II (PIVKA-II), and by abdominal US, dynamic CT scanning, or dynamic MRI every 3 months. Recurrent HCC was diagnosed, using the imaging modalities described earlier, by the appearance of other lesions differed from the primary lesions. The follow-up period was defined as the interval from the date of initial treatment until the date of diagnosis of recurrence or until April 2009 if HCC did not recur.

Statistical analysis. The Pearson product-moment correlation coefficient was used for measuring the linear correlation between 2 continuous variables. Recurrence-free survival was estimated using the Kaplan-Meier method, and differences between curves were examined with a log-rank test. Baseline characteristics were compared using Student's *t* test for continuous variables or the χ^2 test for categorical variables. There were 17 possible predictors for the recurrence of HCC after the initial curative treatment: sex, age, body mass index (BMI), total body fat, amounts of both visceral and subcutaneous fat, the presence of HCV-antibodies (HCV-Ab), Child-Pugh classification, serum albumin concentration, platelet count, homeostasis model assessment of insulin resistance (HOMA-IR = fasting plasma glucose (mg/dL) \times fasting immunoreactive insulin ($\mu\text{U/mL}$)/405), hemoglobin A_{1c} (HbA_{1c}), serum tumor markers (AFP and PIVKA-II), initial treatment for HCC, tumor stage, and serum leptin concentration. Parameters that were significant as determined by univariate analysis were then subjected to multivariate analyses using the Cox proportional hazards model. Statistical significance was defined as $p < 0.05$.

Results

Baseline characteristics and laboratory data of patients.

The baseline characteristics and laboratory data of 85 patients (54 men and 31 women, median age 73 years) are shown in Table 1. The median follow-up period was 484 days (range, 14–1,429 days). Median BMI was 23.2 kg/m², which was classified in the normal range according to the WHO classification of obesity (<http://www.who.int/bmi>). Median free plasma glucose (FPG), free immunoreactive insulin (FIRI), HOMA-IR, and HbA_{1c} were 97 mg/dL, 8.115 $\mu\text{U/mL}$, 2.245, and 5.3%, respectively. The median serum leptin concentration was 5.0 ng/mL (range 1.4–26.6).

Association of the serum leptin concentration with obesity and insulin resistance. Four obesity-related factors were tested for possible association with the serum leptin concentration: BMI, total body fat, and the amounts of visceral and subcutaneous fat (Fig. 1). For BMI analysis, we excluded 7 patients with CT-detected ascites. The Pearson product-moment correlation coefficient and *p* values of BMI and the total body fat with serum leptin concentration were $r = 0.4559$ and $p < 0.0001$, and $r = 0.3560$ and $p = 0.0008$, respectively; indicating that these 2 factors were significantly correlated with the serum leptin concentration. The amount of subcutaneous fat ($r = 0.5174$ and $p < 0.0001$) was also strongly correlated with the serum leptin level, whereas the amount of visceral fat ($r = 0.0987$ and $p = 0.3776$) was not. In addition, no significant correlations were noted between the serum leptin concentration and insulin resistance-related factors, including FPG ($r = -0.0816$ and $p = 0.4579$), FIRI ($r = 0.1049$ and $p = 0.3378$), HOMA-IR ($r = 0.0506$ and $p = 0.6385$), and HbA_{1c} ($r = 0.0194$ and $p = 0.7820$).

Possible risk factors for the recurrence of HCC. In all 33 curative cases of stage I/II HCC, 12 patients experienced recur-

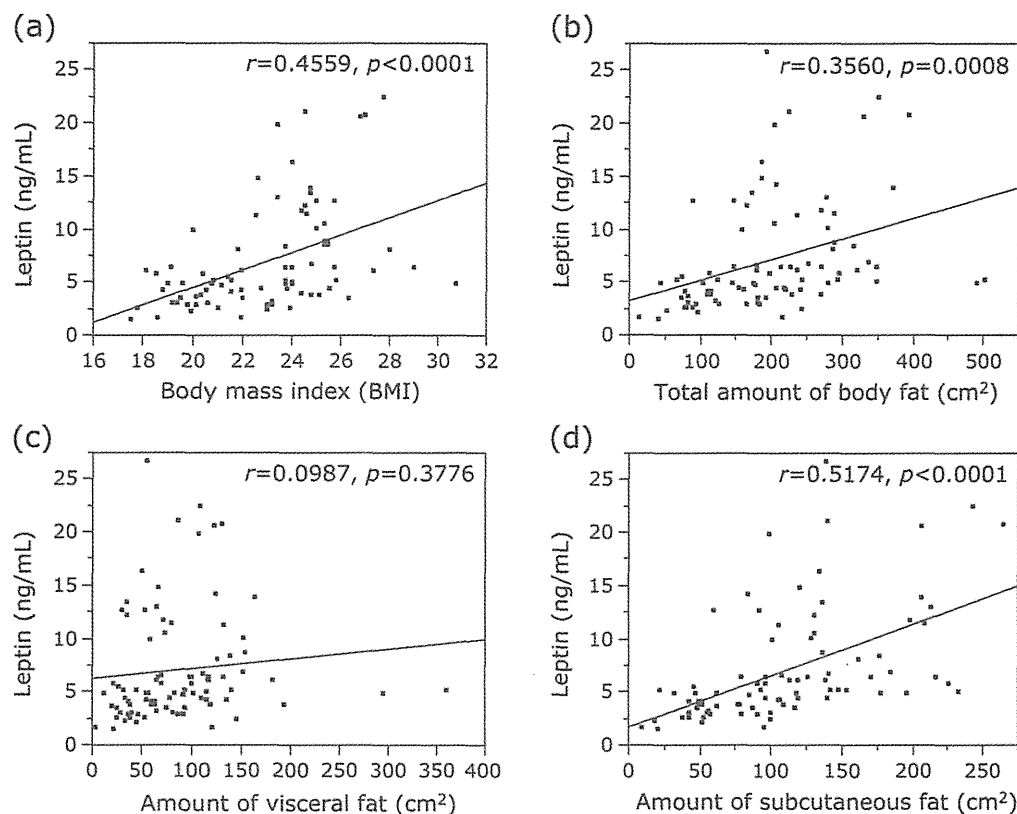


Fig. 1. Correlation between the serum levels of leptin and (a) BMI, (b) total body fat, (c) amount of visceral fat, and (d) amount of subcutaneous fat in patients with HCC ($n = 85$). For BMI analysis, we excluded 7 patients with CT-detected ascites.

rence in the liver, but none exhibited distant metastasis. The 1-year recurrence-free survival in the 33 patients was 79% (Fig. 2a). Fig. 2b shows Kaplan-Meier curves for recurrence-free survival divided into 2 subgroups on the basis of median serum leptin concentration (≤ 5 or > 5 ng/mL), which results in a significant difference ($p = 0.0221$).

The Cox proportional hazards model was used to analyze risk factors for the recurrence of stage I/II HCC after curative treatments using the 17 variables listed in Table 2. BMI (hazard ratio 1.30, 95% CI 1.08–1.56, $p = 0.0062$), total body fat (hazard ratio 1.00, 95% CI 1.00–1.01, $p = 0.0404$), serum albumin concentration (hazard ratio 0.26, 95% CI 0.08–0.81, $p = 0.0210$), AFP (hazard ratio 0.99, 95% CI 0.99–0.99, $p = 0.0365$), and serum leptin concentration (hazard ratio 1.29, 95% CI 1.12–1.50, $p = 0.0003$) were identified as significant risk factors by univariate analysis. Multivariate analysis only identified serum leptin concentration (hazard ratio 1.25, 95% CI 1.07–1.49, $p = 0.0035$) as significant independent risk factor for the recurrence of HCC (Table 3).

Table 4 shows the baseline characteristics and laboratory data of patients divided on the basis of the serum leptin concentration (≤ 5 and > 5 ng/mL). No significant differences were noted between the 2 subgroups, except the amount of subcutaneous fat ($p = 0.0461$).

Discussion

Leptin regulates body weight by signaling information to the brain regarding the availability of energy stored as fat; this

negative feedback loop is disrupted in most obese individuals and results in a state known as leptin resistance.^(16,24) Consistent with the results of previous studies,^(16,24) the serum leptin concentration was significantly correlated with BMI and total body fat in the present study (Fig. 1 a and b). These parameters were also significant risk factors for the recurrence of HCC as determined by univariate analysis (Table 2); however, the serum leptin concentration was the most significant biomarker ($p = 0.0003$).

In addition, we clearly showed for the first time that patients with greater serum leptin concentrations were susceptible to HCC recurrence (Fig. 2b); thus, increased serum leptin levels are a significant independent risk factor for the recurrence of this malignancy (Table 3). This finding indicates that increased serum leptin concentration, which might link obesity with liver carcinogenesis, is a preferable and useful biomarker for screening high-risk groups for the recurrence of HCC. We previously reported that a state of insulin resistance associated with obesity is an independent risk factor for the recurrence of HCC after curative treatment.⁽¹⁰⁾ Furthermore, no significant correlations between serum leptin levels and insulin resistance-related factors were noted in the present study, suggesting these two conditions might be independent from each other in HCC patients. Therefore, a combination evaluation for both the serum leptin level and insulin resistance would be more effective for screening high-risk groups for HCC, and requires future confirmation.

Several studies report that leptin is a risk factor for carcinogenesis at various organ sites, including the liver.^(17–21) Leptin can stimulate cellular proliferation in various types of cancer cells such as HCC cells.^(19–21,25) In addition, when focusing on the liver,

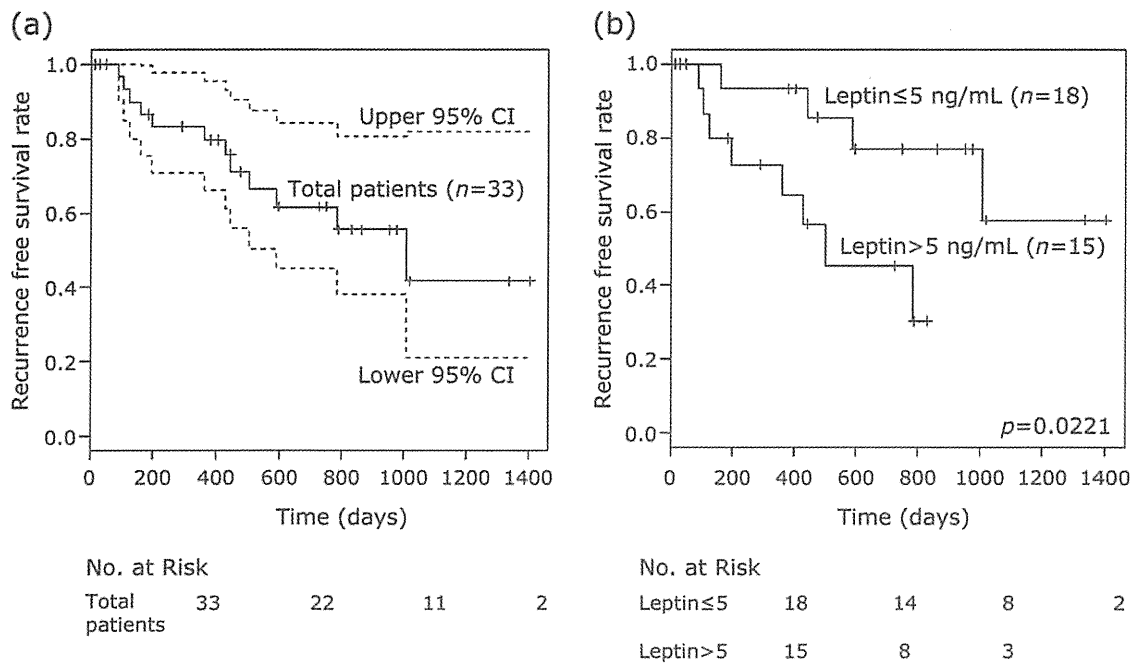


Fig. 2. Kaplan-Meier curves for recurrence-free survival in (a) total patients and in (b) subgroups divided on the basis of the serum leptin concentration (≤ 5 or > 5 ng/mL).

Table 2. Univariate analyses of possible risk factors for recurrence-free survival of HCC using the Cox proportional hazards model

Variable	HR*	95% CI		p value
		lower	upper	
Sex (male vs female)	0.9	0.28	3.09	0.8726
Age (years)	0.96	0.89	1.03	0.277
BMI (kg/m ²)	1.3	1.08	1.56	0.0062
Total body fat (cm ²)	1	1	1.01	0.0404
Amount of visceral fat (cm ²)	1	0.99	1.01	0.0909
Amount of subcutaneous fat (cm ²)	1	0.99	1.01	0.0601
The presence of HCV-Ab (yes vs no)	0.42	0.12	1.98	0.2501
Child-Pugh classification (B + C vs A)	1.33	0.35	4.3	0.6482
ALB (g/dL)	0.26	0.08	0.81	0.021
PLT ($\times 10^4/\mu\text{L}$)	0.87	0.75	1.01	0.0714
HOMA-IR	1.03	0.94	1.1	0.4
HbA _{1c} (%)	0.87	0.37	1.6	0.7108
AFP (ng/mL)	0.99	0.99	0.99	0.0365
PIVKA-II (mAU/mL)	0.99	0.99	1	0.7448
Initial treatment for HCC (RFA vs resection)	1.61	0.42	10.5	0.5128
Stage (II vs I)	1.08	0.32	3.78	0.89
Leptin (ng/mL)	1.29	1.12	1.5	0.0003

*HR represents the values with a unit increase in continuous variables. AFP, α -fetoprotein; BMI, body mass index; CI, confidence interval; HbA_{1c}, hemoglobin A_{1c}; HCC, hepatocellular carcinoma; HCV-Ab, hepatitis C virus antibody; HOMA-IR, homeostasis model assessment of insulin resistance; HR, hazard ratio; PIVKA-II, protein induced by vitamin K absence or antagonists-II; RFA, radiofrequency ablation.

leptin is a potent profibrogenic cytokine and thus plays a key role in the progression of cirrhosis,⁽²⁶⁾ which is a precancerous condition of HCC. Indeed, increased serum leptin concentration has been documented in cirrhotic patients.^(27,28) Moreover, increased leptin expression is associated with increased intratumor micro-

vascular density. Consequently, it is hypothesized that leptin plays a stimulatory role in the development of HCC via neovascularization.⁽²⁹⁾ In addition to using leptin as a biomarker for the risk of HCC recurrence, the present findings suggest that targeting leptin might be an effective strategy for the prevention and treatment of

Table 3. Multivariate analyses of possible risk factors for recurrence-free survival of HCC using the Cox proportional hazards model

Variable	HR*	95% CI		p value
		lower	upper	
BMI (kg/m ²)	1.2	0.83	1.81	0.3278
Total body fat (cm ²)	1	0.99	1.01	0.8003
ALB (g/dL)	0.54	0.12	2.28	0.4018
AFP (ng/mL)	0.99	0.99	1	0.1416
Leptin (ng/mL)	1.25	1.07	1.49	0.0035

*HR represents the values with a unit increase in continuous variables. AFP, α -fetoprotein; BMI, body mass index; CI, confidence interval; HR, hazard ratio.

Table 4. Baseline demographic and clinical characteristics of patients classified on the basis of the serum leptin concentration

Variable	Leptin \leq 5 ng/mL (n = 18)	Leptin > 5 ng/mL (n = 15)	p value
Sex (male/female)	13/5	6/9	0.0604
Age (years)	72.5 [59–87]	70 [50–85]	0.2565
BMI (kg/m ²)	21.5 [17.8–30.7]	24.5 [18.5–27.7]	0.1111
Total body fat (cm ²)	167.5 [73.9–490.9]	207.3 [112.2–350.8]	0.2591
Amount of visceral fat (cm ²)	69.4 [19.9–294.4]	98.9 [21.9–181.6]	0.9479
Amount of subcutaneous fat (cm ²)	90.2 [42.0–232.3]	134.3 [79.6–242.5]	0.0461
Etiology (C/others)	14/4	11/4	0.767
Child-Pugh classification (A/B/C)	15/3/0	10/5/0	0.2657
ALB (g/dL)	3.6 [2.6–4.2]	3.3 [2.4–4.4]	0.2708
PLT ($\times 10^4/\mu\text{L}$)	12.45 [7.7–26.1]	9.5 [3.0–20.6]	0.0895
FPG (mg/dL)	97.5 [83–271]	105 [75–154]	0.7424
FIRI ($\mu\text{U}/\text{mL}$)	6.05 [2.57–65.2]	14.3 [7.3–27.4]	0.3657
HOMA-IR	1.51 [0.53–24.8]	3.41 [1.45–9.40]	0.641
HbA _{1c} (%)	5.3 [4.5–10.3]	5.2 [3.7–6.8]	0.3351
Stage (I/II)	7/11	9/6	0.2253
Initial treatment for HCC (resection/RFA)	6/12	2/13	0.1726
AFP (ng/mL)	8 [0–20500]	28 [1–2530]	0.1687
PIVKA-II (mAU/mL)	22.7 [8–201000]	26 [7–29800]	0.4385

Values are median [range]. AFP, α -fetoprotein; C, hepatitis C virus; FPG, fasting plasma glucose; FIRI, fasting immunoreactive insulin; HbA_{1c}, hemoglobin A_{1c}; HCC, hepatocellular carcinoma; HOMA-IR, homeostasis model assessment of insulin resistance; PIVKA-II, protein induced by vitamin K absence or antagonists-II; RFA, radiofrequency ablation.

HCC. Ribatti *et al.* state that anti-leptin antibodies reduce the angiogenic response in HCC biopsy specimens.⁽²⁹⁾ Decreases in serum leptin are also associated with the prevention of obesity-related liver tumorigenesis in obese and diabetic mice models.⁽¹⁴⁾

In conclusion, we report that patients with high serum leptin concentrations are susceptible to HCC recurrence in stage I/II cases curatively treated by surgical resection or RFA. Increased serum leptin concentration may be a useful biomarker for predicting the recurrence of HCC in high-risk patients.

Acknowledgments

This work was supported in part by Grants-in-Aid from the Ministry of Education, Science, Sports and Culture of Japan (No. 22790638 to M. S. and No. 21590838 to H. M.) and by Grant-in-Aid for the 3rd Term Comprehensive 10-Year Strategy for Cancer Control from the Ministry of Health, Labour and Welfare of Japan.

Abbreviations

AFP	α -fetoprotein
BMI	body mass index
CT	computed tomography
DM	diabetes mellitus
FPG	fasting plasma glucose
FIRI	fasting immunoreactive insulin
HbA _{1c}	hemoglobin A _{1c}
HBV	hepatitis B virus
HCC	hepatocellular carcinoma
HCV	hepatitis C virus
HOMA-IR	homeostasis model assessment of insulin resistance
LCSGJ	Liver Cancer Study Group of Japan
MRI	magnetic resonance imaging
PIVKA-II	protein induced by vitamin K absence or antagonists-II
RFA	radiofrequency ablation
TACE	transarterial chemoembolization
TAI	transarterial infusion
US	ultrasonography

References

- 1 El-Serag HB. Hepatocellular carcinoma: an epidemiologic view. *J Clin Gastroenterol* 2002; **35**: S72–S78.
- 2 Toyama T, Hiramatsu N, Yakushijin T, *et al.* A new prognostic system for hepatocellular carcinoma including recurrent cases: a study of 861 patients in a single institution. *J Clin Gastroenterol* 2008; **42**: 317–322.
- 3 Gomaa AI, Khan SA, Toledano MB, Waked I, Taylor-Robinson SD. Hepatocellular carcinoma: epidemiology, risk factors and pathogenesis. *World J Gastroenterol* 2008; **14**: 4300–4308.
- 4 Koike Y, Shiratori Y, Sato S, *et al.* Risk factors for recurring hepatocellular carcinoma differ according to infected hepatitis virus: an analysis of 236 consecutive patients with a single lesion. *Hepatology* 2000; **32**: 1216–1223.
- 5 Ikeda K, Saitoh S, Tsubota A, *et al.* Risk factors for tumor recurrence and prognosis after curative resection of hepatocellular carcinoma. *Cancer* 1993; **71**: 19–25.
- 6 Adachi E, Maeda T, Matsumata T, *et al.* Risk factors for intrahepatic recurrence in human small hepatocellular carcinoma. *Gastroenterology* 1995; **108**: 768–775.
- 7 Nagashima I, Hamada C, Naruse K, *et al.* Surgical resection for small hepatocellular carcinoma. *Surgery* 1996; **119**: 40–45.
- 8 Ishii H, Okada S, Nose H, *et al.* Predictive factors for recurrence after percutaneous ethanol injection for solitary hepatocellular carcinoma. *Hepato-gastroenterology* 1996; **43**: 938–943.
- 9 Muto Y, Sato S, Watanabe A, *et al.* Overweight and obesity increase the risk for liver cancer in patients with liver cirrhosis and long-term oral supplementation with branched-chain amino acid granules inhibits liver carcinogenesis in heavier patients with liver cirrhosis. *Hepato Res* 2006; **35**: 204–214.
- 10 Imai K, Takai K, Nishigaki Y, *et al.* Insulin resistance raises the risk for recurrence of stage I hepatocellular carcinoma after curative radiofrequency ablation in hepatitis C virus-positive patients: a prospective, case series study. *Hepato Res* 2010; **40**: 376–382.
- 11 El-Serag HB, Tran T, Everhart JE. Diabetes increases the risk of chronic liver disease and hepatocellular carcinoma. *Gastroenterology* 2004; **126**: 460–468.
- 12 Caldwell SH, Crespo DM, Kang HS, Al-Osaimi AM. Obesity and hepatocellular carcinoma. *Gastroenterology* 2004; **127**: S97–S103.
- 13 Park EJ, Lee JH, Yu GY, *et al.* Dietary and genetic obesity promote liver inflammation and tumorigenesis by enhancing IL-6 and TNF expression. *Cell* 2010; **140**: 197–208.
- 14 Iwasa J, Shimizu M, Shiraki M, *et al.* Dietary supplementation with branched-chain amino acids suppresses diethylnitrosamine-induced liver tumorigenesis in obese and diabetic C57BL/KsJ-db/db mice. *Cancer Sci* 2010; **101**: 460–467.
- 15 Maeda K, Okubo K, Shimomura I, Mizuno K, Matsuzawa Y, Matsubara K. Analysis of an expression profile of genes in the human adipose tissue. *Gene* 1997; **190**: 227–235.
- 16 Maffei M, Halaas J, Ravussin E, *et al.* Leptin levels in human and rodent: measurement of plasma leptin and ob RNA in obese and weight-reduced subjects. *Nat Med* 1995; **1**: 1155–1161.
- 17 Wang XJ, Yuan SL, Lu Q, *et al.* Potential involvement of leptin in carcinogenesis of hepatocellular carcinoma. *World J Gastroenterol* 2004; **10**: 2478–2481.
- 18 Stattin P, Palmqvist R, Söderberg S, *et al.* Plasma leptin and colorectal cancer risk: a prospective study in Northern Sweden. *Oncol Rep* 2003; **10**: 2015–2021.
- 19 Hardwick JC, Van Den Brink GR, Offerhaus GJ, Van Deventer SJ, Peppelenbosch MP. Leptin is a growth factor for colonic epithelial cells. *Gastroenterology* 2001; **121**: 79–90.
- 20 Somasundar P, Riggs D, Jackson B, Vona-Davis L, McFadden DW. Leptin stimulates esophageal adenocarcinoma growth by nonapoptotic mechanisms. *Am J Surg* 2003; **186**: 575–578.
- 21 Tsuchiya T, Shimizu H, Horie T, Mori M. Expression of leptin receptor in lung: leptin as a growth factor. *Eur J Pharmacol* 1999; **365**: 273–279.
- 22 Kobayashi J, Tadokoro N, Watanabe M, Shinomiya M. A novel method of measuring intra-abdominal fat volume using helical computed tomography. *Int J Obes Relat Metab Disord* 2002; **26**: 398–402.
- 23 Liver Cancer Study Group of Japan. The general rules for the clinical and pathological study of primary liver cancer. *Jpn J Surg* 1989; **19**: 98–129.
- 24 Knight ZA, Hannan KS, Greenberg ML, Friedman JM. Hyperleptinemia is required for the development of leptin resistance. *PLoS One* 2010; **5**: e11376.
- 25 Chen C, Chang YC, Liu CL, Liu TP, Chang KJ, Guo IC. Leptin induces proliferation and anti-apoptosis in human hepatocarcinoma cells by up-regulating cyclin D1 and down-regulating Bax via a Janus kinase 2-linked pathway. *Endocr Relat Cancer* 2007; **14**: 513–529.
- 26 Leclercq IA, Farrell GC, Schriemer R, Robertson GR. Leptin is essential for the hepatic fibrogenic response to chronic liver injury. *J Hepatol* 2002; **37**: 206–213.
- 27 Henriksen JH, Holst JJ, Møller S, Brinch K, Bendtsen F. Increased circulating leptin in alcoholic cirrhosis: relation to release and disposal. *Hepatology* 1999; **29**: 1818–1824.
- 28 Ockenga J, Bischoff SC, Tillmann HL, *et al.* Elevated bound leptin correlates with energy expenditure in cirrhotics. *Gastroenterology* 2000; **119**: 1656–1662.
- 29 Ribatti D, Belloni AS, Nico B, *et al.* Leptin-leptin receptor are involved in angiogenesis in human hepatocellular carcinoma. *Peptides* 2008; **29**: 1596–1602.

Entecavir and interferon- α sequential therapy in Japanese patients with hepatitis B e antigen-*positive* chronic hepatitis B

Masaru Enomoto · Shuhei Nishiguchi · Akihiro Tamori · Sawako Kobayashi · Hiroki Sakaguchi · Susumu Shiomi · Soo Ryang Kim · Hirayuki Enomoto · Masaki Saito · Hiroyasu Imanishi · Norifumi Kawada

Received: 8 April 2012 / Accepted: 5 July 2012 / Published online: 2 August 2012
© Springer 2012

Abstract

Background The outcomes of sequential therapy with lamivudine followed by interferon have been unsatisfactory in Japanese patients with hepatitis B envelope antigen (HBeAg)-*positive* chronic hepatitis B. However, the efficacy of sequential therapy with entecavir and interferon remains unclear.

Methods Twenty-four HBeAg-*positive* patients (23 men and 1 woman; mean age 39 ± 7 years) received entecavir 0.5 mg alone for 36–52 weeks, followed by entecavir plus interferon- α for 4 weeks, and lastly by interferon- α alone for 20 weeks. Twenty-three patients had genotype C infection, and one had genotype A infection.

Results No entecavir-resistant mutant variants emerged in any patient. Hepatitis flare occurred in three patients during

interferon- α treatment after the withdrawal of entecavir, but none had hepatic decompensation. Serum hepatitis B surface antigen levels did not change during or after therapy. Serum hepatitis B core-related antigen levels were significantly decreased at the start ($P < 0.0001$) and at the end of interferon- α treatment ($P < 0.0001$), but returned to baseline levels after treatment. Twenty-four weeks after the completion of the sequential therapy, a sustained biochemical, virological, and serological response was achieved in 5 (21 %) patients. The proportion of patients in whom HBeAg was lost during entecavir treatment was significantly higher among those with a sustained response than among those with no response ($P = 0.015$).

Conclusions The rate of response to sequential therapy with entecavir and interferon- α in Japanese patients with HBeAg-*positive* chronic hepatitis B was not higher than the rate in previous studies of lamivudine followed by interferon.

Keywords Chronic hepatitis B · Genotypes · Interferon- α · Entecavir · Sequential therapy

For the B-SHOT Study Group.

Other members of the B-SHOT Study Group are listed in the Appendix.

M. Enomoto · A. Tamori · S. Kobayashi · H. Sakaguchi · N. Kawada (✉)

Department of Hepatology, Osaka City University Graduate School of Medicine, 1-4-3 Asahimachi, Abeno-ku, Osaka 545-8585, Japan
e-mail: kawadanori@med.osaka-cu.ac.jp

S. Nishiguchi · H. Enomoto · M. Saito · H. Imanishi
Department of Internal Medicine, Hyogo College of Medicine, Hyogo, Japan

S. Shiomi
Department of Nuclear Medicine, Osaka City University Graduate School of Medicine, Osaka, Japan

S. R. Kim
Department of Gastroenterology, Kobe Asahi Hospital, Hyogo, Japan

Introduction

Infection with hepatitis B virus (HBV) remains an important public health problem and a leading cause of liver-related morbidity worldwide [1, 2]. The natural course of chronic HBV infection acquired perinatally or during infancy consists of three distinct phases: ‘immune tolerant’, ‘immune reactive’, and ‘inactive carrier’. During the immune-reactive phase, rises in alanine aminotransferase (ALT) are attributable to the host’s immune response to HBV, and the occurrence of hepatitis will eventually be followed by spontaneous seroconversion from hepatitis B

envelope antigen (HBeAg) to anti-HBe. HBeAg seroconversion usually results in clinical remission and a life-long inactive state; however, patients with persistently detectable HBeAg and high HBV DNA levels who have recurrent hepatitis flares are at increased risk of developing cirrhosis and hepatocellular carcinoma [3, 4].

Currently available antiviral treatment for chronic hepatitis B includes nucleos(t)ide analogues such as lamivudine, adefovir, entecavir, and tenofovir, and the immunomodulator interferon [5–7]. The direct, potent antiviral effects of nucleos(t)ide analogues induce biochemical and virological responses in most patients, but viral relapse and exacerbations of hepatitis commonly occur after discontinuation of treatment. Long-term use of nucleos(t)ide analogues is associated with the emergence of drug-resistant variants possessing mutations in the HBV polymerase gene. In contrast, interferon-induced remission of chronic hepatitis B is durable, but is achieved in only a minority of patients. In randomized controlled trials, concomitant treatment with lamivudine and interferon- α has offered little clinical benefit, in terms of the rates of sustained therapeutic response, as compared with interferon- α alone [8, 9].

Serfaty et al. [10] reported that sequential therapy with lamivudine followed by interferon- α was effective in patients with chronic hepatitis B. In their pilot study in France, sustained virological and biochemical response was achieved in 8 (57 %) of the 14 patients who received lamivudine 100 mg alone for 20 weeks, followed by interferon- α 5 MU 3 times/week plus lamivudine for 4 weeks, and lastly by interferon- α alone for 24 weeks [10]. Some other groups have studied similar protocols for sequential therapy, but results have been conflicting [11–17]. The inconsistent results may have been caused, at least in part, by differences in the included HBV genotypes among studies, because HBV genotypes have specific geographic distributions and can affect the response to interferon [18, 19]. In our previous study [14], the rate of response to sequential therapy with lamivudine and interferon in 24 Japanese HBeAg-positive patients with chronic HBV genotype C infection was 29 %, considerably lower than the rate reported by Serfaty et al. [10].

Randomized controlled trials have shown that entecavir has higher antiviral activity against HBV than lamivudine [20, 21]. Among licensed nucleos(t)ide analogues, entecavir is used as a first-line treatment of choice for chronic hepatitis B, similar to tenofovir disoproxil fumarate [22]. Use of a potent nucleoside analogue before the initiation of interferon may improve the outcomes of sequential therapy.

In this study, we evaluated the efficacy of sequential therapy with entecavir and interferon- α in Japanese patients with HBeAg-positive chronic hepatitis B. In addition to the

monitoring of serum HBeAg and HBV DNA levels, serum hepatitis B surface antigen (HBsAg) and hepatitis B core-related antigen (HBcrAg) [23, 24] levels were monitored during and after sequential therapy. The clinical characteristics of patients who had a sustained response to the sequential therapy were compared with those of patients who had no response.

Patients and methods

Patients

The subjects were 24 Japanese patients with HBeAg-positive chronic hepatitis B (23 men and 1 woman; mean age 39 ± 7 years) who had received sequential therapy with entecavir alone and then entecavir plus interferon- α followed by interferon- α alone between September 2006 and August 2011. The inclusion criteria were as follows: (1) persistent or fluctuating elevations of serum ALT levels for at least 6 months before the start of therapy; (2) presence of HBsAg in serum; (3) presence of HBeAg and absence of anti-HBe; (4) presence of HBV DNA $>10^5$ copies/mL (equivalent to 20,000 IU/mL); (5) no use of corticosteroids or immunomodulatory drugs, including interferon, within 1 year before the start of therapy; (6) no use of nucleos(t)ide analogues, such as lamivudine, within 1 year before the start of therapy; (7) absence of resistance to nucleos(t)ide analogues; (8) absence of antibodies to hepatitis C virus and other likely causes of chronic liver disease; and (9) no clinical signs of decompensated cirrhosis or hepatocellular carcinoma. The study procedures were in accordance with the Helsinki Declaration of 1975 (1983 revision) and were approved by the ethics committee of each participating center. Written informed consent was obtained from each patient. This study was registered in the UMIN Clinical Trials Registry (registration ID number, UMIN000000808).

Treatment

Patients were treated with entecavir alone for 36–52 weeks, followed immediately by both entecavir and interferon- α for 4 weeks, and lastly by interferon- α alone for 20 weeks. Entecavir (Baraclude; Bristol-Myers, Tokyo, Japan) was given orally at a dose of 0.5 mg once daily. Natural interferon- α (Otsuka Pharmaceutical, Tokyo, Japan) was given by intramuscular injection, at a dose of 5 MU, three times a week for 24 weeks (a protocol commonly used in Japan during the study period). All patients were followed up for at least 24 weeks after the completion of treatment, and responses to therapy were assessed as follows: *biochemical response* was defined as a decrease in